NRC Research Press

ARTICLE

On two species of *Riocypris* (Crustacea, Ostracoda) from northern Patagonia and their relation to *Eucypris fontana*: implications in paleoenvironmental reconstructions

C.A. Coviaga, A.P. Pérez, L.Y. Ramos, P. Alvear, and G.C. Cusminsky

Abstract: Two species of ostracods new to Patagonia, Argentina, are described. One of them, ***Riocypris whatleyi*** sp. nov., is described for the first time, and the second, ***Riocypris sarsi*** (Daday, 1902) comb. nov., is reallocated from genus *Eucypris* to genus *Riocypris*. Inter- and intra-specific variations in shape, size, and sexual dimorphism were evaluated based on geometric morphometric analysis. Moreover, morphological and morphometric comparative analyses were applied to re-examine living and quaternary specimens recovered from previous studies. Based on these results, a generic reassignment for the Patagonian *Eucypris fontana* (Jurine, 1820) into the genus *Riocypris* is proposed. Contributing to the knowledge on the systematic and autecology of this enigmatic species, widely distributed in Patagonia and frequently used in paleolimnological reconstructions, generates science-based evidence for their use as indicator species. Additionally, our results emphasize the usefulness of studying the living representatives (i.e., with valves and appendages) for elucidating the taxonomic status of the individual specimens, especially those present in paleontological records and used as bioproxies in paleolimnological studies.

Key words: Ostracoda, paleoecology, Patagonia, *Riocypris whatleyi*, *Riocypris sarsi*.

Résumé : Deux espèces d'ostracodes observées pour la première fois en Patagonie (Argentine) sont décrites. Une d'elles, ***Riocypris whatleyi*** sp. nov., est décrite pour la première fois, et l'autre, ***Riocypris sarsi*** (Daday, 1902) comb. nov., est réaffectée du genre Eucypris au genre *Riocypris*. Des variations interspécifiques et intraspécifiques de la forme, de la taille et du dimorphisme sexuel ont été évaluées à la lumière d'une analyse morphométrique géométrique. En outre, des analyses morphologiques et morphométriques comparatives ont été employées pour réexaminer des spécimens vivants et du Quaternaire récupérés d'études antérieures. À la lumière de ces résultats, une réaffectation générique pour l'*Eucypris fontana* (Jurine, 1820) patagonien au genre *Riocypris* est proposée. Cette contribution aux connaissances sur la systématique et l'autécologie de cette espèce énigmatique à vaste répartition en Patagonie et fréquemment utilisée dans des reconstitutions paléolimnologiques produit des données basées sur la science pour appuyer son utilisation comme espèce indicatrice. Nos résultats soulignent en outre l'utilité d'étudier les représentants vivants (c.-à-d. avec leurs valves et appendices) pour élucider le statut taxonomique des spécimens individuels, en particulier ceux qui sont présents dans des registres paléontologiques et qui sont utilisés comme bioindicateurs dans des études paléolimnologiques. [Traduit par la Rédaction]

Mots-clés : ostracodes, paléoécologie, Patagonie, *Riocypris whatleyi*, *Riocypris sarsi*.

Introduction

Ostracods are one of the most diverse crustacean taxa, abounding in both marine and freshwater and even in (semi-) terrestrial environments. There are about 2000 living nonmarine species belonging to around 200 genera worldwide (Martens et al. 2008; Martens and Savatenalinton 2011). From these, about 300 species have been recorded in the Neotropical region (Martens et al. 2008; Martens and Savatenalinton 2011; Martens et al. 2013). In Argentinian Patagonia, there are approximately 33 documented taxa (Schwalb et al. 2002; Cusminsky et al. 2005; Ramón-Mercau et al. 2012; Ramón-Mercau and Laprida 2016; Coviaga et al. 2018). In this region, taxonomic studies on nonmarine ostracods started at the beginning of the 20th century, with the first descriptions conducted by Vavrá (1898) and Daday (1902). Beginning in the 1990s, studies of this type were reinitiated, focusing on the fossil fauna of Río Negro province, where Cusminsky and Whatley (1996) reported five new species. These taxa were later recognized in quaternary sequence from Patagonia (lakes Cari-Laufquen Grande, Cardiel, and Cháltel), allowing the identification of variations in the hydrology of the watersheds along the Upper Pleistocene – Holocene (Whatley and Cusminsky 2000; Markgraf et al. 2003; Cusminsky et al. 2011; Ohlendorf et al. 2014; Coviaga et al. 2017). Research on the extant fauna in nonmarine environments from Patagonia began in the 20th century, parallel to the study of fossil ostracods (Ramón-Mercau et al. 2012; Díaz and Martens 2014; Coviaga 2016; Coviaga et al. 2018).

Nonmarine ostracods are increasingly used to interpret past paleolimnology and paleoclimatology. In this sense, it is of utmost importance to study the taxonomy and ecology of extant faunas to allow trustworthy informed extrapolations from the present to

Received 19 August 2017. Accepted 16 March 2018.

C.A. Coviaga,* L.Y. Ramos, and G.C. Cusminsky. INIBIOMA, CONICET – Universidad Nacional del Comahue, Quintral 1250, San Carlos de Bariloche, Argentina.
A.P. Pérez. Photobiology Laboratory, INIBIOMA, CONICET – Universidad Nacional del Comahue, San Carlos de Bariloche, Argentina.
P. Alvear. INIBIOMA, CONICET, San Carlos de Bariloche, Argentina.
Corresponding author: Corina A. Coviaga (email:corinacoviaga@gmail.com).
*Present address: Delegación de Geología y Petróleo; INIBIOMA, CONICET – Universidad Nacional del Comahue, Quintral 1250, Bariloche, Argentina.

Fig. 1. Locality map indicating the lakes where *Riocypis whatleyi* sp. nov. and *Riocypris sarsi* comb. nov. were collected; i.e., Los Juncos, El Toro, and La Vertiente. The sampled lakes were highlighted with red stars online (grey stars in print). Additionally, insets with details were added showing the size, shape, and surrounding topography of the lakes (lake images taken from Google Earth, free version). Colour version online.

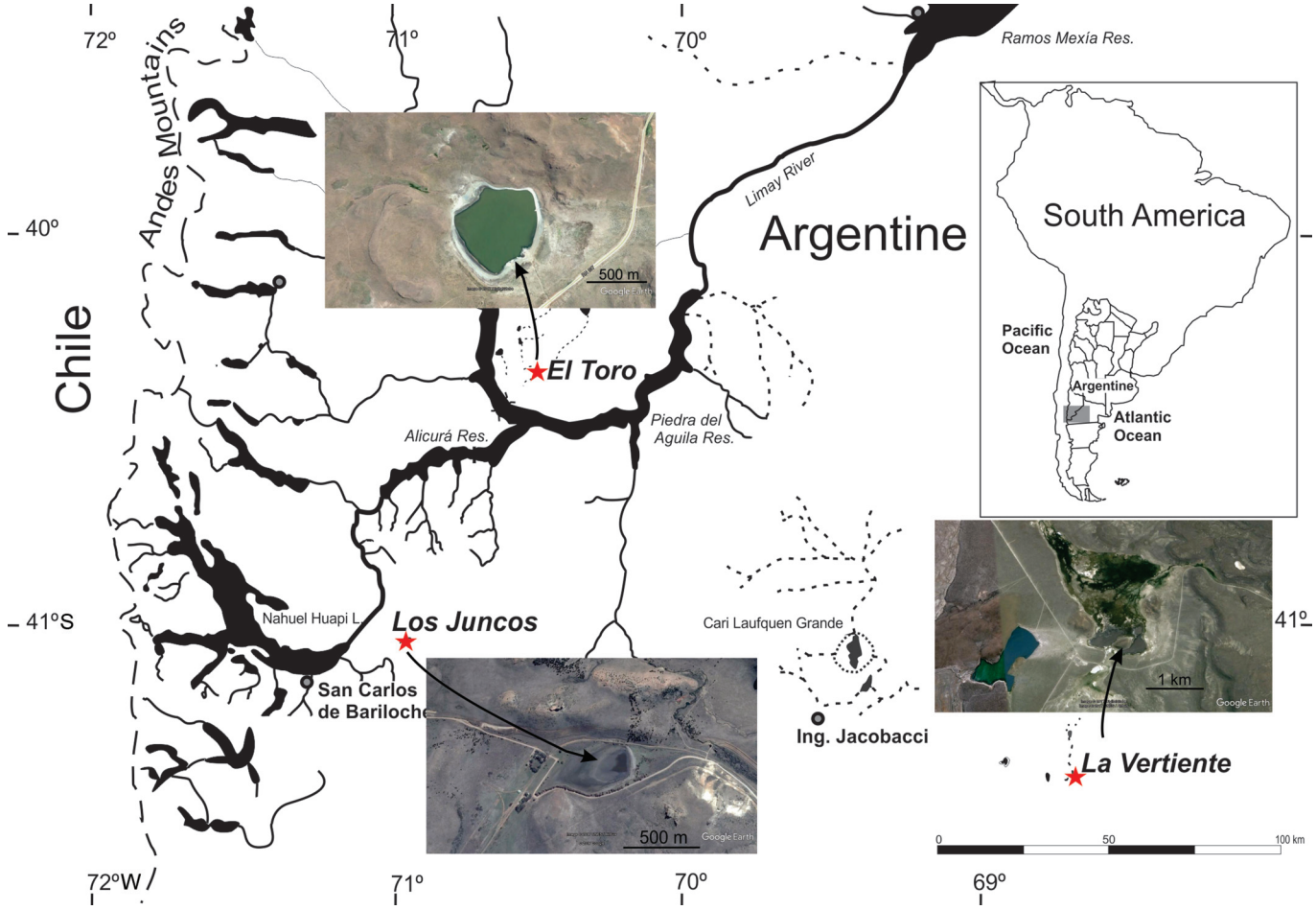

the past (Torres Saldarriaga and Martínez 2010; Mischke et al. 2010; Zhang et al. 2013; Coviaga et al. 2018). Particularly in northern Patagonia, a recent survey carried out in 40 aquatic environments has shown that of the 22 identified species, 8 species are present in Quaternary sequences from Patagonia (Coviaga et al. 2018). This highlights the potential use of these organisms as tools in paleoenvironmental interpretations for the region, and at the same time, the need of a proper taxonomic determination of species, with its consequent consensus among researchers (Coviaga 2016). Only in this way will it be possible to make precise and correct comparisons and interpretations possible, both about fossil and extant ostracod fauna. The taxonomic identification from paleontological records, based only on fossil remains, is often complex (Torres Saldarriaga and Martínez 2010). In this context, the analysis of extant representatives (i.e., with valves and appendages) provides a convenient tool for elucidating the taxonomic status of individual specimens (Coviaga 2016). Here we (*i*) describe two species of the genus *Riocypris* Klie, 1935, from three shallow lakes in northern Patagonia; (*ii*) re-examined fossil material from four lacustrine sequences, including two cores from lakes where *Riocypris* species have been sampled alive; and (*iii*) repositioned those Patagonian *Eucypris fontana* (Graf, 1931) into the genus *Riocypris*. Comparative analyses were performed based on the morphological disparity of both appendages and valves. Moreover, geometric morphometric analyses on valves was used to support the taxonomical analysis of valves and the reassignment of Patagonian *E. fontana* fossils. A taxonomic key to the species level is proposed, and the records of species from the Patagonian region described here are discussed, especially with regards to its use in paleoenvironmental studies.

Materials and methods

Ostracod specimens

The material examined was collected during austral spring (November and December) of the years 2012, 2013, and 2015 from the lakes La Vertiente (41°30′24″S, 68°37′38″W; 930 m above sea level (asl)), El Toro (40°19′14″S, 70°25′13″W; 1021 m asl), and Los Juncos (41°03′32″S, 71°00′31″W; 909 m asl), northern Patagonia, Argentina (Fig. 1). All samples were taken with a 200 μm mesh sized plankton hand-net dragged along the water–sediment interface, in a 1–6 m long transect, depending on the environment (Schaffer et al. 1994), and preserved in 50% ethanol. Given that the environments studied are very shallow (maximum depth 0.6 ± 0.3 m), using this sampling method allowed us to recover most ostracods crawling in the sediments, as well as those swimming in the water column (Coviaga et al. 2018). During field surveys, around midday, electrical conductivity, temperature, dissolved oxygen, pH, and depth were measured at the bottom of the water column and the habitat type was recorded.

At the laboratory, within 24 h after sampling, ostracods were concentrated and transferred to 70% ethanol for permanent storage. The specimens were sorted, measured, and dissected under stereoscopic microscopes (Olympus SZ30 and SZ61 and Nikon

SMZ-645). The limb morphology was analysed under a light microscope and drawings of soft parts were made using a camera lucida (Olympus BX40 and BX50). Images of ostracod valves were obtained with a scanning electron microscope (Phillips SEM 515, CNEA Bariloche, Argentina). The valves were stored dry in micropaleontological slides, whereas soft parts were mounted on glass slides with Hydromatrix® (Micro-Tech-Lab, Austria) mounting medium and covered with a cover slip. Specimens that were not dissected were sorted by species and were preserved in 70% ethanol. For comparison, several Holocene male and female valves previously assigned as *Eucypris fontana* (Graf 1931) in the literature (Cusminsky and Whatley 1996; Whatley and Cusminsky 1999; Cusminsky et al. 2011; Coviaga 2016; Coviaga et al. 2017) were studied. These fossils were recovered from sedimentary sequences from lakes El Toro (40°19′14″S, 70°25′13″W; Coviaga et al. 2017), Cari-Laufquen Grande Outcrop (41°08′S, 69°28′W; Cusminsky et al. 2011; Coviaga 2016), Los Juncos (41°03′32″S, 71°00′31″W; Cusminsky and Whatley 1996), and Río Maquinchao Outcrop (41°09′S, 69°25′W; Whatley and Cusminsky 1999; Cusminsky et al. 2011). All examined material (holotypes and paratypes) of the two new species were stored at the Micropaleontological collection of the Centro Regional Universitario Bariloche, Universidad Nacional del Comahue (UNC-PMIC: Universidad Nacional del Comahue – Colección de Paleontología–Microfósiles) under the collection numbers UNC-PMIC 131–150.

The ostracod identification was carried out on adult specimens, based both on valves and body appendages, following Cusminsky and Whatley (1996), Meisch (2000), Cusminsky et al. (2005), and Karanovic (2008, 2012). Nomenclature proposed by Broodbakker and Danielopol (1982), adapted for the A2 by Martens (1987) and for the T3 by Meisch (2000), was used in the description of chaetotaxy of soft parts. For higher taxonomical orders, the system proposed by Horne et al. (2002) was employed.

The following abbreviations are used in the text and figures:

Sites — ET = El Toro; ETC = El Toro Core; LV = La Vertiente; MO = Maquinchao Outcrop; CLGO = Cari-Laufquén Outcrop; LJ = Los Juncos; LJC = Los Juncos Core.

Valves — Cp = carapace; valves: H = height, L = length, W = width; LV = left valve; RV = right valve; CIL = calcified inner lamella.

Limbs and soft parts — A1 = antennula; A2 = antenna; Md = mandible; RLO = rake-like organ; Mx = maxillula; T1 = first thoracic limb; Lpp = left prehensile palp; Rpp = right prehensile palp; T2 = second thoracic limb; T3 = third thoracic limb; CR = caudal ramus; CRa = attachment of caudal ramus; vb = ventral branch of CR; dv = dorsal branch of CR. Values are expressed in micrometres (μm) as the arithmetic mean ± standard deviation (with the minimum and maximum values shown in parentheses); *n* = number of individuals.

Morphometric analyses of valves

For the analysis of valve shape of *Riocypris* species, geometric morphometric techniques were applied following Baltanás and Danielopol (2011) and Neubauer and Linhart (2008). Left valves were photographed in external lateral view with a digital camera (AmScope MD500) fitted to a stereomicroscope (×20 magnification; Olympus SZH10 equipped with an APO objective lens IX). Outlines of 114 valves of *Riocypris whatleyi* sp. nov. (LV: *n* = 24; ET: *n* = 74), including females and males, and *Riocypris sarsi* comb. nov. (LJ: *n* = 16), including only females, were digitized using TpsDig software (Rohlf 2010). To compare these outlines, geometric morphometric analysis was performed using Linhart's B-spline algorithm with Morphomatica version 1.6 software (Linhart et al. 2007; Neubauer and Linhart 2008). Thirty-two control points (16 dorsal and 16 ventral) were necessary to accurately reconstruct the outline of each specimen (the maximum error of the reconstructed shape compared with the original outline was below 1%). The shape differences between any two outlines were estimated as the area deviation, which is the area between the outlines once they were superimposed. Previously, outlines were normalized for position, rotation, and size (normalized to unit area) (Neubauer and Linhart 2008). To visualize and characterize the main shape and size differences, virtual mean outlines (consensus shape) for each species were computed. The matrix of pairwise differences was used as input for non-metric multidimensional scaling (n-MDS) analysis to evaluate dissimilarities in valve shape. Additionally, statistical differences in valve shape between species, populations, and sexes were tested by performing a one-way ANOSIM (analysis of similarity) (Clarke and Warwick 2001). Multivariate statistical analysis of pairwise differences between valve outlines were carried out with PRIMER version 6 software (Clarke and Gorley 2006).

To examine size differences, maximum valve length and height were measured on the valve images using AmScope software. Given that both length and height were highly correlated ($r_{Pearson} = 0.95$, $p < 0.05$), the following analyses were performed only using valve length. The size differences between *R. whatleyi* and *R. sarsi* were evaluated using a Student's *t* test. Subsequently, to test the effect of site and sex on valve size of *R. whatleyi*, a factorial ANOVA followed by Tukey's test was carried out using STATISTICA version 7.0 software (StatSoft, Inc. 2004). Assumptions of normality and homoscedasticity were previously evaluated using the Lilliefors and Bartlett tests, respectively.

Additionally, the valves previously assigned to *E. fontana* in the sedimentary sequences, i.e., El Toro (*n* = 10), Cari-Laufquen Grande Outcrop (*n* = 3), Los Juncos (*n* = 10), and Río Maquinchao Outcrop (*n* = 3), were analysed following the same procedure as the extant specimens. For shape comparison with *Riocypris* species described in this study, the *E. fontana* outlines were included into the n-MDS analysis (Cusminsky and Whatley 1996; Cusminsky et al. 2011; Coviaga et al. 2017).

Results

Systematic results

Class	Ostracoda Latreille, 1802
Subclass	Podocopa Sars, 1866
Order	Podocopida Sars, 1866
Family	Cyprididae Baird, 1845
Subfamily	Cyprinotinae Bronstein, 1947
Genus	*Riocypris* Klie, 1935

TYPE SPECIES: *Riocypris uruguayensis* Klie, 1935 by original designation.

DIAGNOSIS FOR THE GENUS (MODIFIED AFTER KARANOVIC 2012): Right valve with inwardly displaced selvage at least anteriorly. Selvage on the left valve, if present, usually peripherical. Inner list prominent, especially on the left valve. Third segment of antennule elongated. Maxillular palp cylindrical. Prehensile palps asymmetrical, c seta absent on protopod of first thoracopod. d1 seta on walking leg considerably longer (usually three times) than d2, penultimate segment on the same leg clearly divided. Penultimate segment on cleaning leg with only one seta. Caudal ramus slender and elongated, both claws (Ga and Gp) and setae (Sa and Sp) present, posterior seta not transformed into claw. Attachment simple.

Riocypris whatleyi sp. nov.
(Figs. 2A–2L, 3A–3E, 4A–4E, 5A–5F)

Eucypris fontana (Graf, 1931). Cusminsky and Whatley 1996, pl. 2, fig. 9.
Eucypris fontana (Graf, 1931). Schwalb et al. 2002, pl. 1, figs. 6, 8.
Eucypris fontana (Graf, 1931). Cusminsky et al. 2005, pl. 1, figs. 16, 17, 19.
Eucypris fontana (Graf, 1931). Ramos et al. 2015, fig. 3.
Eucypris fontana (Graf, 1931). Coviaga et al. 2017.
Eucypris fontana (Graf, 1931). Coviaga et al. 2018, figs. 2H–2I.

Fig. 2. (A–N) *Riocypris whatleyi* sp. nov. and (O–X) *Riocypris sarsi* comb. nov. (A) RV, ev (UNC-PMIC 134, male). (B) RV, ev, detail of anteroventral zone (UNC-PMIC 134, male). (C) RV, ev (UNC-PMIC 132, female). (D) RV, ev (UNC-PMIC 148, female). (E) Cp, dv (UNC-PMIC 137, male). (F) Cp, dv, detail of anterodorsal zone (UNC-PMIC 137, male). (G) LV, iv (UNC-PMIC 135, male). (H) LV, iv, detail of posteroventral zone (UNC-PMIC 135, male). (I) LV, iv, detail of anteroventral zone (UNC-PMIC 135, male). (J) LV, iv, detail of internal wart-like elevations (UNC-PMIC 135, male). (K) RV, iv (UNC-PMIC 135, male). (L) RV, iv, detail of anteroventral zone (UNC-PMIC 135, male). (M) RV, iv (UNC-PMIC 150). (N) RV, iv, detail of anteroventral zone (UNC-PMIC 150). (O) Cp, dv (UNC-PMIC 147, female). (P) Cp, dv, detail of anterodorsal zone (UNC-PMIC 147, female). (Q) LV, ev (UNC-PMIC 144, female). (R) LV, ev, detail of anteroventral zone (UNC-PMIC 144, female). (S) LV, ev, detail of external wart-like elevation (UNC-PMIC 144, female). (T) RV, iv (UNC-PMIC 145, female). (U) RV, iv, detail of anteroventral zone (UNC-PMIC 145, female). (V) LV, iv (UNC-PMIC 145, female). (W) LV, iv (UNC-PMIC 146, female). (X) LV, iv, detail of anteroventral zone (UNC-PMIC 146, female). Scale bars: A–I, K–R, T–X = 200 μm, J = 20 μm, and S = 10 μm. For abbreviations refer to the Materials and methods.

ZOOBANK NO.: These descriptions were submitted on 11 July 2018. The ZooBank number for *Riocypris whatleyi* is urn:lsid:zoobank.org:act:9CC33CA6-1878-41B1-AA7E-AA50055E1F58. The manuscript ZooBank number is urn:lsid:zoobank.org:pub:FC75A935-3F57-4A59-9148-466BE48BB2C9.

TYPE LOCALITY: Lake La Vertiente, Río Negro province (41°30′24″S, 68°37′38″W; 930 m asl), Argentina.

STUDIED MATERIAL: *Holotype* — One dissected male from Lake La Vertiente, with valves stored dry in a micropaleontological slide and dissected soft parts mounted in a permanent slide with Hydromatrix® mounting medium. Collection number: UNC-PMIC 131. *Paratypes* — Specimens from Lake La Vertiente. Two ovigerous females and three males, with valves used for SEM and stored in micropaleontological slides and dissected soft parts kept in sealed slides (UNC-PMIC 132–136); one carapace used for SEM and stored in micropaleontological slides (UNC-PMIC 137). *Other material dissected, used for description and illustration* — Sixteen ovigerous females and 13 males from Lake La Vertiente (41°30′24″S, 68°37′38″W; 930 m asl); 2 ovigerous females and 2 males (UNC-PMIC 148–150) from El Toro (40°19′14″S, 70°25′13″W; 1021 m asl).

ETYMOLOGY: In honour of Robin Whatley for his invaluable contribution to the knowledge of the Quaternary and extant ostracods in Patagonia, Argentina.

DIAGNOSIS: Large individuals (L = 1790–1470 μm). Carapace subtriangular, with greatest height in the middle. Right valve with anterior selvage inwardly displaced, left valve with selvage marginal. Left valve overlaps right valve along all margins. Valves surface smooth, with a row of four wart-shaped elevations along the anterior margin. These wart-like elevations are also present inside both valves. A1 with dorsobasal seta reaching the third segment. Natatory setae of A2 well developed, exceeding tips of terminal claws. Mx with serrated tooth bristles on the third endite. Length of seta d1 on T2 around five times longer than distal d2.

DESCRIPTION OF ADULT MALE (FIGS. 2A–2H): Large individuals, around 1600 μm in length. Carapace subtriangular in lateral view. Greatest height at the middle of the valve, around 60% of length. Dorsal margin arched, anterior margin broadly rounded, posterior margin slightly straight to narrowly rounded in the posteroventral margin. Ventral margin straight to almost concave (Figs. 2A, 2B). In dorsal view, carapace subelliptical, with greatest width around middle, equalling 50% of length; anterior margin acute and posterior one rounded (Fig. 2E). Left valve overlaps right valve along anterior, ventral, and posterior margins. In ventral view, left valve overlaps slightly to right valve in the middle of the carapace. Valve surface smooth with hair mainly in anterior end and normal pores along the carapace. A row of four wart-shaped elevations along the anterior margin and marginal pores are also present (Fig. 2B). Seminal tube scars are present in the posteroventral margin. Right valve slightly smaller than left valve.

In interior view, inner lamella broad in the anterior margin turned to narrow along the ventral and posterior margins. Left valve with selvage peripheral all around margins, inner list well developed anteriorly, much less posteriorly (Figs. 2G–2I). Right valve with salvage displaced internally all around free margins and without well-developed inner list. Line of concrescence distinctive and vestibule broad, especially in the anterior margin (Figs. 2K, 2L). Hinge adont, formed by a sulcus in VI and a bar in VD. Inner wart-like elevations present in both valves (Fig. 2J). Muscle scar typical of the superfamily Cyprididae, located in the central area of the carapace (Fig. 2G).

A1 (Fig. 3A) — With seven articulated segments. Basal segment with one dorsal seta reaching the third segment and two unequally long ventral setae. Second segment with one anterior seta, passing the middle of following segment. Rome and Wouters organs not seen. Third segment elongated, with two unequal setae, one short posterior and one long anterior, extending beyond the terminal segment. Fourth segment with two long anterior setae and two unequal posterior setae. Fifth and sixth segments with four long swimming setae. Alpha seta on the apical part of the sixth segment was not seen. Terminal segment with one aesthetasc, y_a nine times longer than terminal segment, two long swimming setae, and one shorter seta.

A2 (Fig. 3B) — Second segment of protopodite with one long ventral seta. First segment of endopodite with a medioventral aesthetasc Y and the exopodite reduced into two short and one long setae. At distal end of this segment, the five swimming setae extending slightly beyond tips of terminal claws. The sixth seta among them reaching the distal end of terminal segment. Penultimate segment medially with two setae on exterior side and four setae on ventral side (t1-4). Sexual dimorphism in chaetotaxy of penultimate segment, males with z1 and z2 large and equal claws, z3 a long seta, beyond tips of terminals claws. G1 a small claw (more than four times the length of the terminal segment), G2 a long claw, and G3 a small seta (slightly shorter than G1). Terminal segment with claw GM well developed and almost reaching tip of other claws, Gm very slender and less than half length of GM, seta g and aesthetasc y3 with a seta fused at the base of this aesthetasc. Aesthetasc y3 three times longer than final segment.

Md — With strong coxa bearing six–seven cuspate teeth (Fig. 3D). Palp (Fig. 3E) with both S setae plumose well developed. One long seta and α seta bare and short. Second segment dorsally with a group of three unequally long apical setae, ventrally with three long and smooth setae, one shorter accompanying seta, and the β seta, the latter slender and plumose. Penultimate segment with four unequally long setae dorsally, one long and one short smooth setae ventrally, and in lateral side and apically, three long setae and the γ seta, the latter short, stout, and covered with short setulae. Terminal segment with three claws and two unequal setae.

RLO (Fig. 4A) — T-shaped with seven teeth.

Mx (Fig. 4B) — Maxillular palp two-segmented. Penultimate segment with six long setae and one short seta (situated on opposite side from long ones). Terminal segment of palp cylindrical, approximately two times longer than wide, set with four claws. Two large bristles on third endite slightly serrated. Both sideways-directed bristles present.

T1 (Figs. 4C, 4D, 4E) — Protopod with 2 a setae, and b and d setae with endite bearing 10 apical plumose setae and 2 subapical smooth setae. Endopod transformed into two asymmetrical prehensile palps. The right one (Fig. 4E) with stronger finger than the left one (Fig. 4D). First segment of the Rpp subapically with one short sensory organ, second segment stout, apically with one sensory organ. Lpp basal segment with one stout subapical sensory

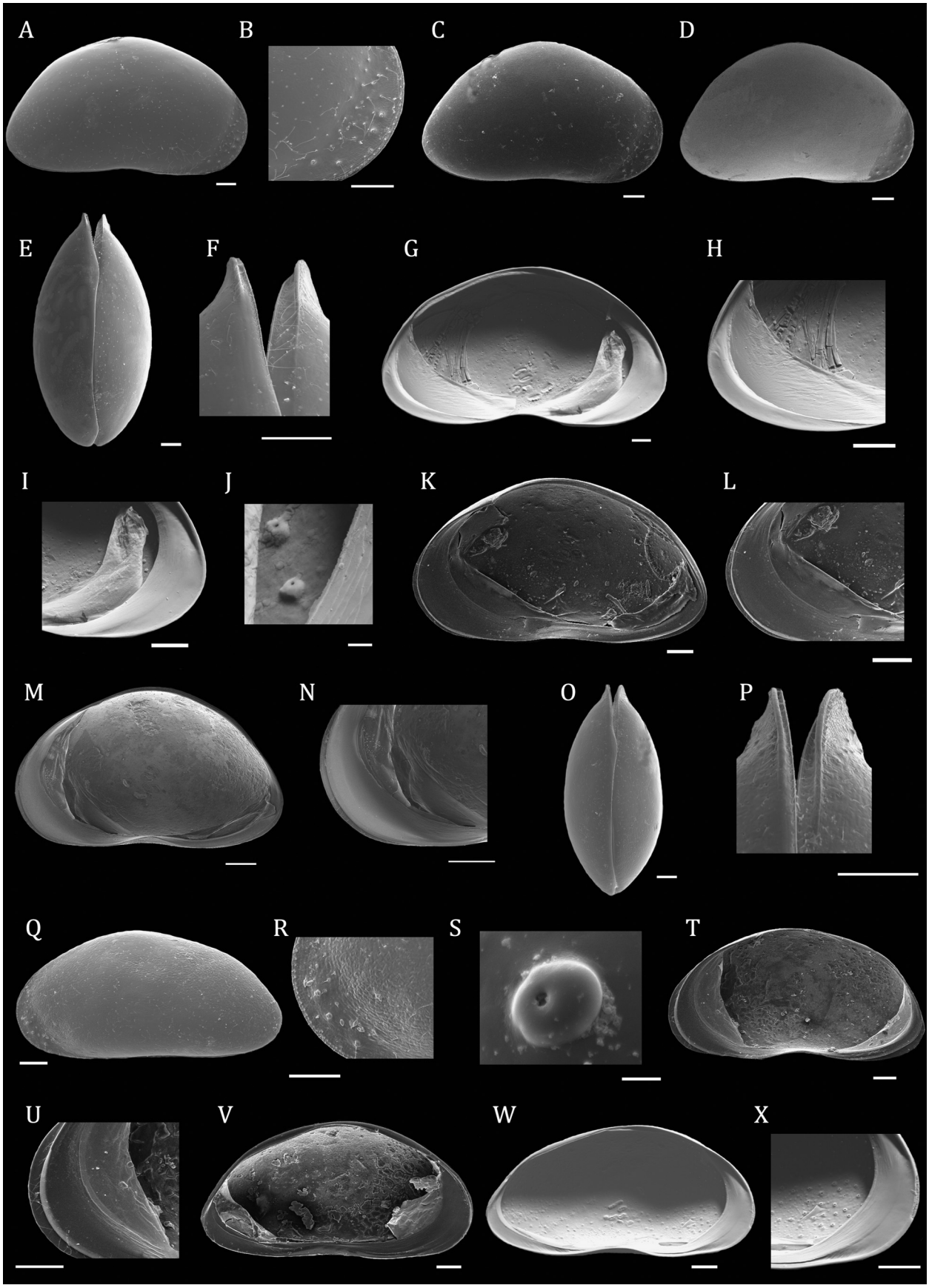

Fig. 3. *Riocypris whatleyi* sp. nov. (A) A1 (UNC-PMIC 131, male). (B) A2 (UNC-PMIC 136, male). (C) A2 (UNC-PMIC 135, female). (D) Md Cx (UNC-PMIC 132, male). (E) Md palp (UNC-PMIC 131, male). Scale bar = 100 μm. For abbreviations refer to the Materials and methods.

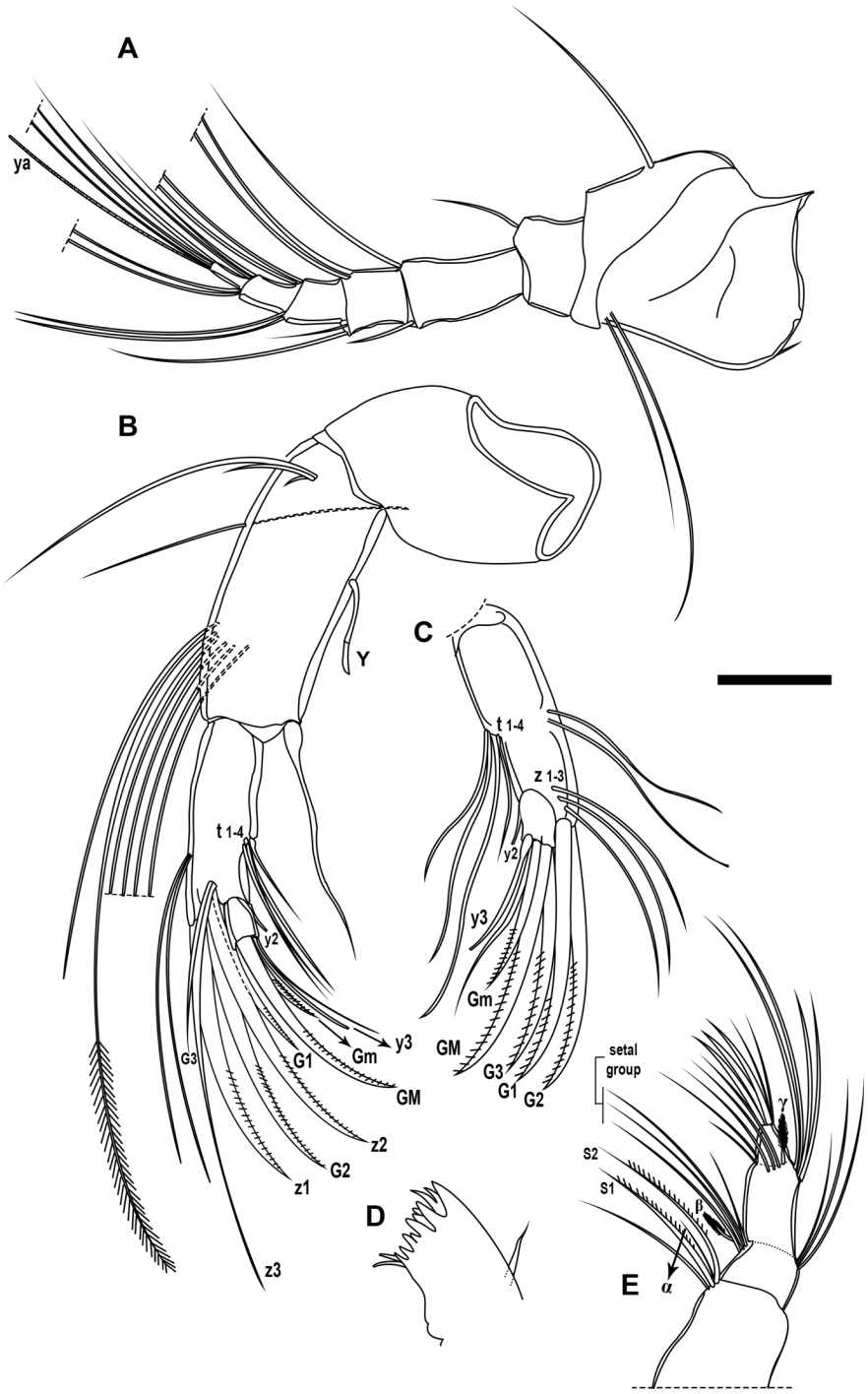

organ; second segment relatively slender, apically with one sensory organ.

T2 (Fig. 5C) — Basal segment with proximal seta d1 around five times longer than distal d2. Second segment with long seta (e), exceeding the distal end of following segment. Seta (f) on third segment reaching the terminal segment. Fourth segment with two unequal g setae. Terminal segment with two apical setae (h1 and h3) and a well-developed, long, serrated claw (h2).

T3 (Fig. 5D) — Cleaning leg with three long setae (d1, d2, and dp) in basal segment. The second one with one long apical seta (e). Penultimate segment with one medial seta (f). Terminal segment with an apical pincer organ with two curved modified setae (h1 and h2) and one subapical seta (h3).

CR (Fig. 5F) — Symmetrical, nearly straight. Posterior edge smooth. The anterior (Ga) and posterior (Gp) claws serrated, with the Ga being 1.6 as long as the Gp. Anterior seta (Sa) slightly shorter than posterior. CRa (Fig. 5E) with well-developed vb and very short db; main branch slightly curved.

Hemipenis (Fig. 5A) — Symmetrical, with tips of outer and middle lobes separated. Middle lobe large and blunt; outer lobe

Fig. 4. *Riocypris whatleyi* sp. nov. (A) RLO (UNC-PMIC 131, male). (B) Mx (UNC-PMIC 133, male). (C) T1 (UNC-PMIC 135, female). (D) Rpp (UNC-PMIC 135, male). (E) Lpp (UNC-PMIC 135, male). Scale bar = 100 μm. For abbreviations refer to the Materials and methods.

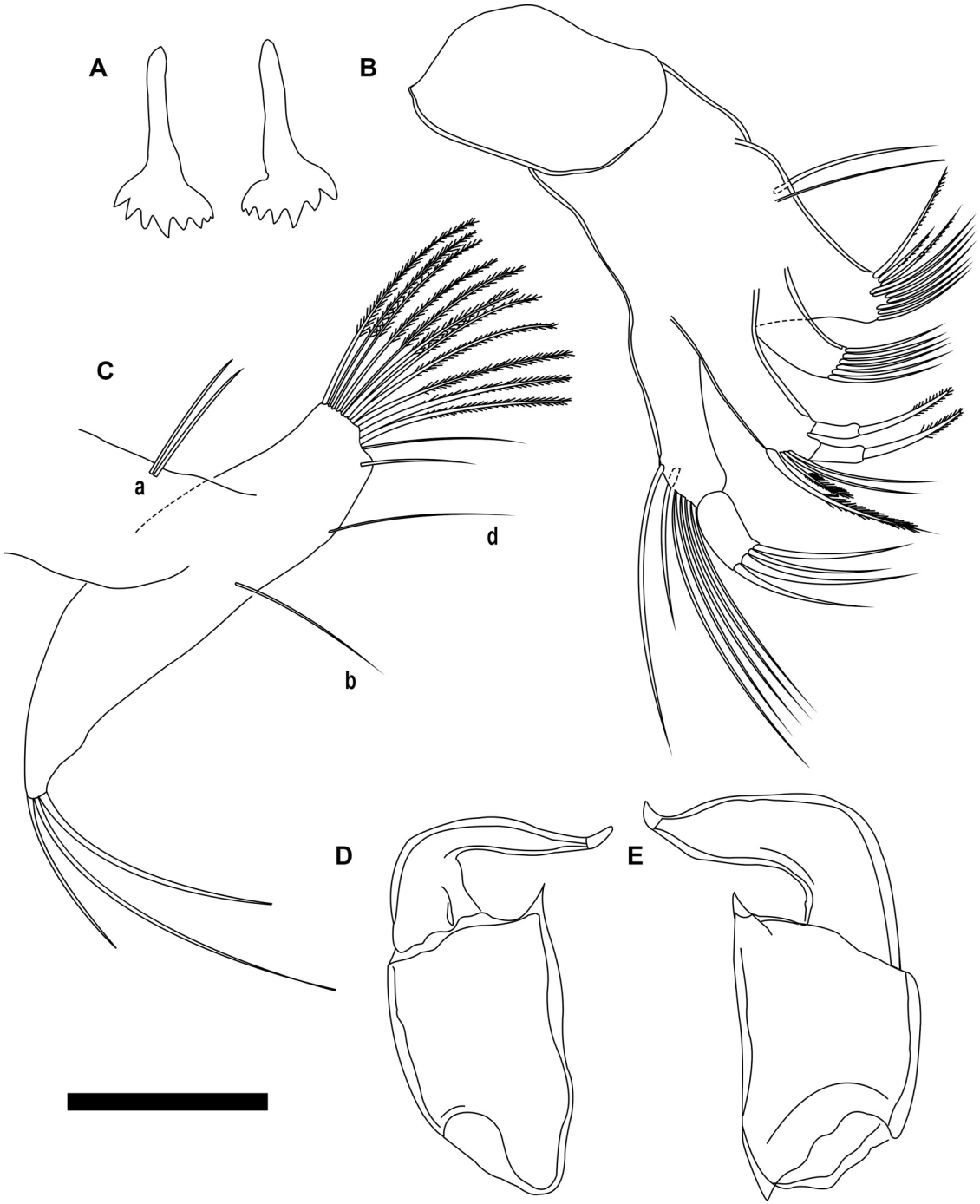

smaller and curved, distally bluntly pointed and reaching the end of the middle lobe. Zenker's organ muscular with numerous internal spines (Figs. 5B, 6).

DESCRIPTION OF ADULT FEMALE (FIGS. 2C, 2D, 3C, 4C): Female carapace larger, with dorsal margin slightly more convex than male (Figs. 2C, 2D). Other shape features same as in the male.

A1, Md, Mx, T2, T3, and caudal ramus similar to those of adult male.

A2 (Fig. 3C) — Penultimate segment with all three z setae long and all claws well developed and subequally long.

T1 (Fig. 4C) — Protopod with 2 a setae, and b and d setae with endite bearing 10 apical plumose setae and 2 subapical smooth setae. With endopodite asymmetrical, undivided palp three unequal apical setae, two short and in the middle one long seta.

Measurements (in μm) as follows:

UNC-PMIC 131: L = 1562, H = 914.
UNC-PMIC 132: L = 1602, H = 939.
UNC-PMIC 133: L = 1648, H = 972.
UNC-PMIC 134: L = 1524, H = 897.
UNC-PMIC 135: L = 1470, H = 896.
UNC-PMIC 136: L = 1499, H = 903.
UNC-PMIC 137: L = 1556, W = 764.

LV — Males: L = 1518 ± 32, H = 900 ± 16 (n = 9). Females: L = 1572 ± 44, H = 940 ± 29 (n = 15).

Fig. 5. *Riocypris whatleyi* sp. nov. (A) Hemipene (UNC-PMIC 134, male). (B) Zenker's organ (UNC-PMIC 132, male). (C) T2 (UNC-PMIC 131, male). (D) T3 (UNC-PMIC 131, male). (E) CRa (UNC-PMIC 131, male). (F) CR (UNC-PMIC 131, male). Scale bar = 100 μm. For abbreviations refer to the Materials and methods.

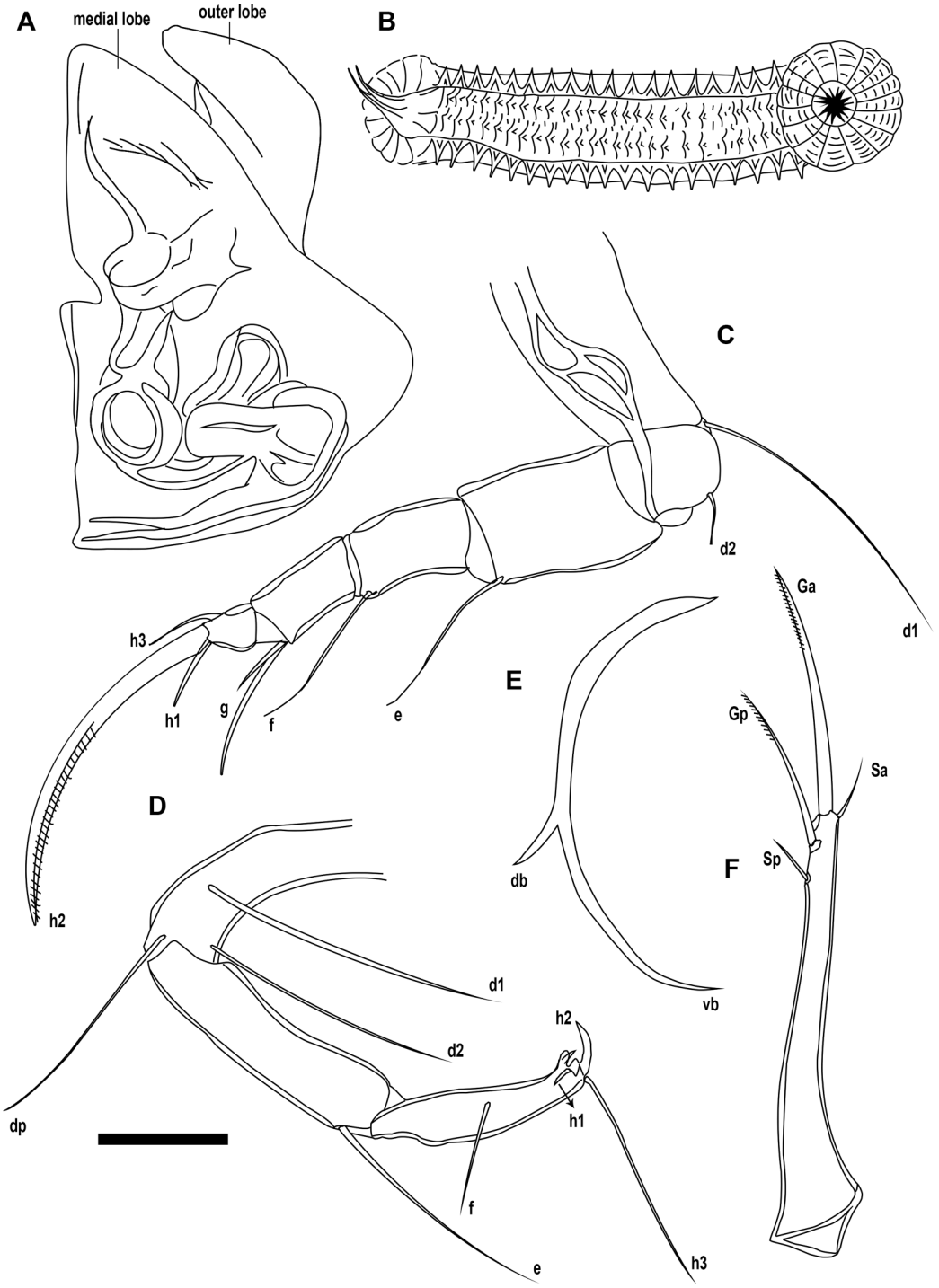

ET — Males: L = 1600 ± 34, H = 959 ± 22 (*n* = 38). Females: L = 1729 ± 30, H = 1049 ± 23 (*n* = 36).

DISTRIBUTION AND ECOLOGY: *Riocypris whatleyi* has been found in two Patagonian shallow lakes: La Vertiente (a permanent and vegetated environment) and El Toro (a semipermanent lake without vegetation). La Vertiente presented pH values around 8.6, temperate waters (17.8 °C), moderate conductivity (1.5 mS/cm), and a dissolved oxygen concentration of 10.6 mg/L. El Toro was characterized by alkaline pH values (9.2 ± 0.6), temperatures from 15.0 to 21.0 °C, conductivity from 0.8 to 42.4 mS/cm, and dissolved oxygen from 10.0 to 13.0 mg/L. These values were recorded during the austral spring (November and December) of the years 2013–2015, around midday.

REMARKS: *Riocypris whatleyi* differs from *R. uruguayensis* in the shape of the carapace. The carapace of the latter is triangular in lateral view, with a lower H/L ratio (0.52 ± 0.00 (*n* = 2) in *R. uruguayensis*

Fig. 6. *Riocypris whatleyi* sp. nov., male Zenker's organ. Scale bar = 100 μm. Colour version online.

and 0.60 ± 0.01 (n = 98) in *R. whatleyi*); the dorsal margin more arched and the ventral margin more concave. In dorsal view, the carapace is distinctly beak-shaped on the anterior region. *Riocypris uruguayensis* has the short sixth seta of the second A2 endopodal segment shorter, projecting beyond of the middle of the penultimate segment, whereas in *R. whatleyi*, this seta reaches the distal end of the last segment. Additionally, in *R. uruguayensis*, the penultimate A2 segment is densely haired at its distal ventral corner, with setae on the ventral side finely spiked in the last 2/3 of its length. In *R. uruguayensis*, Sa on the caudal ramus shorter, around 1/6 of length of Ga, whereas in *R. whatleyi*, it is around 1/4 of the length of Ga. Caudal ramus with setulae on anterior margin in *R. uruguayensis*. Additionally, in this species, Sp shorter (1/5 of the length of Gp), being shorter than the distance between Sp and Gp.

Riocypris whatleyi differs from *Riocypris hinzeae* Karanovic, 2008 in the shape of the carapace; subrectangular in lateral view, with anterior and posterior ends rounded and dorsal margin almost flat in the latter. Additionally, the A1 in *R. hinzeae* has the anterior seta of the second segment shorter, the third segment more elongated and with one very short anterior seta. The last segment of the Mx palp is more elongated (three times longer than wide in *R. hinzae* and two times longer than wide in *R. whatleyi*), the relationship d1/d2 in T2 is smaller (approximately three times in *R. hinzeae* and five times in *R. whatleyi*), and the Sa on the caudal ramus is very short, around 1/7 of length of Ga (the Sa is around 1/4 of the length of Ga in *R. whatleyi*).

Riocypris sarsi comb. nov.
(Figs. 2O–2X, 7A–7E, 8A–8E)

Eucypris sarsii (Daday, 1902). Daday 1902, tab. XV, figs. 1–7; figs. 2*a*–2*c*.

Eucypris sarsi (Dady, 1902). Farkas 1972, figs. 1–5.

Eucypris fontana (Graf, 1931). Cusminsky and Whatley 1996, pl. 2, figs. 10–12.

Eucypris fontana (Graf, 1931). Cusminsky et al. 2005, pl. 1, fig. 18.

ZOOBANK NO.: These descriptions were submitted on 11 July 2018. The ZooBank number for *Riocypris sarsi* is urn:lsid:zoobank.org:act:FB71EA26-BE61-46B3-810E-0686BF455140. The manuscript ZooBank number is urn:lsid:zoobank.org:pub:FC75A935-3F57-4A59-9148-466BE48BB2C9.

STUDIED MATERIAL: Six ovigerous females dissected from Lake Los Juncos, with valves stored dry in a micropaleontological slide and dissected soft parts mounted in a permanent slide with Hydromatrix® mounting medium (UNC-PMIC 138–143). Three ovigerous, dissected females, with valves used for SEM and stored in micropaleontological slides and dissected soft parts kept in sealed slides (UNC-PMIC 144–146); one carapace used for SEM and stored in micropaleontological slides (UNC-PMIC 147). Besides the aforementioned specimens, three females were collected, measured, and dissected.

DIAGNOSIS AFTER DADAY (1902): Large individuals, about 1450 μm long. Carapace elongated in lateral view, greatest height situated 1/3 from anterior of the valve. Right valve with anterior selvage inwardly displaced, left valve with selvage marginally. Left valve overlaps right valve along all margins. Valve surface smooth with a row of four wart-shaped elevations along the anterior margin. These wart-like elevations also present inside of both valves.

First segment of A1 with one dorsal seta reaching the second segment. Natatory setae of A2 well developed, distinctly exceeding tips of terminal claws. Mx with serrated tooth bristles on the third endite. Length of seta d1 on T2 around four times longer than distal d2.

DESCRIPTION OF ADULT FEMALE (FIGS. 2O–2X): Large individuals, around 1450 μm in length. Carapace elongated in lateral view. Greatest height situated just anteriorly of the middle of the valve, equalling approximately 50% of length. Dorsal margin weakly arched and ventral margin slightly concave, anterior end broadly rounded, and posterior end slightly blunted (Figs. 2Q, 2V, 2W). In dorsal view, carapace subelliptical with the greatest width around middle, equalling 45% of length; anterior margin acute and posterior

margin blunted (Figs. 2O, 2P). Left valve overlaps right valve along anterior, ventral, and posterior margins. In ventral view, left valve slightly overlaps to right valve in the middle of the carapace. Valve surface smooth with hair mainly in anterior end and normal pores along the carapace (Fig. 2Q). A row of four wart-shaped elevations along the anterior margin and marginal pores are also present (Figs. 2R, 2S). Right valve slightly smaller than left valve.

In interior view, inner lamella broad in the anterior margin turned to narrow along the ventral and posterior margin. Left valve, with selvage peripheral all around margins, inner list well developed anteriorly, much less posteriorly (Figs. 2V–2X). Right valve with selvage displaced internally all around free margins and well-developed inner list anteriorly (Figs. 2T, 2U). Line of concrescence distinctive and vestibule broad, especially in the anterior margin. Hinge adont, formed by a sulcus in VI and a bar in VD. Inner wart-like elevations present in both valves. Muscle scar typical of the superfamily Cyprididae, located in the central area of the carapace (Fig. 2W).

A1 (Fig. 7A) — With seven articulated segments. Basal segment with one dorsal seta reaching the second segment and two unequally long ventral setae. Second segment with one anterior seta, reaching the middle of following segment; Rome and Wouters organs not seen. Third segment elongated with two unequal setae, the longer reaching the distal end of the following segment. Fourth segment with two long anterior and two unequal posterior setae. Fifth and sixth segments with four long swimming setae. Alpha seta on the apical part of the sixth segment was not seen. Terminal segment with one aesthetasc, y_a, two long swimming setae and one shorter seta. Aesthetasc 13 times longer than terminal segment.

A2 (Fig. 7B) — Second segment of protopodite with one long ventral seta. First segment of endopodite with a medioventral aesthetasc Y and the exopodite reduced into two short and one long seta. At distal end of this segment, the five swimming setae reaching tip of terminal claws. The sixth seta among them reaching the distal end of penultimate segment. Penultimate segment medially with two setae on exterior side and four setae on ventral side (t1-4). Distally with three long z setae and three (G1–G3) claws well developed and subequally long. Terminal segment with claw GM well developed and almost reaching tip of other claws; Gm shorter, passing middle of GM; a long g seta and the aesthetasc y3, the latter approximately four times longer than final segment.

Md — With strong coxa bearing six–seven cuspate teeth (Fig. 7C). Palp (Fig. 7D) with both S setae plumose well developed. One long seta and α seta bare and short. Second segment dorsally with a group of three long apical setae; ventrally with three long and smooth setae, one short accompanying seta, and a slender β seta, the last two plumose. Penultimate segment with four unequally long setae dorsally; one long and one short smooth setae ventrally, and in lateral side and apically, three long setae and the γ seta short, stout, and covered with short setulae. Terminal segment with three claws and two unequal setae.

RLO (Fig. 7E) — T-shaped with seven teeth.

Mx (Fig. 8A) — Maxillular palp two-segmented. Penultimate segment with six long setae and one short seta (situated on opposite side from long ones). Terminal segment of palp cylindrical, almost three times longer than width, set with four claws. Two large bristles on third endite serrated. Both sideways-directed bristles present.

T1 (Fig. 8B) — Protopod with 2 a setae, and b and d setae with endite bearing 15 plumose, unequal apical setae. Endopodite palp symmetrical, with three unequal apical setae, two short and one long.

T2 (Fig. 8C) — Basal segment with proximal seta d1 approximately four times longer than distal d2. Second segment with long seta (e), exceeding the distal end of following segment. Seta (f) on third segment beyond the distal end of terminal segment. Fourth segment with two unequal g setae. Terminal segment with two apical setae (h1 and h3) and a well-developed, long, serrated claw (h2).

T3 (Fig. 8D) — Cleaning leg with three long setae (d1, d2, and dp) in basal segment. The second one with one long apical seta (e). Penultimate segment with one medial seta (f). Terminal segment with an apical pincer organ with two curved modified setae (h1 and h2) and one subapical seta (h3).

CR (Fig. 8F) — Symmetrical, nearly straight. Posterior edge smooth. The anterior (Ga) and posterior (Gp) claws serrated, with Ga being two times as long as Gp. Sa slightly longer than Sp. CRa (Fig. 8E) with well-developed vb and very short db; main branch slightly curved.

Measurements (in μm) as follows:

UNC-PMIC 138: L = 1536, H = 812.
UNC-PMIC 139: L = 1505, H = 818.
UNC-PMIC 140: L = 1534, H = 819.
UNC-PMIC 141: L = 1562, H = 815.
UNC-PMIC 142: L = 1508, H = 802.
UNC-PMIC 143: L = 1585, H = 845.
UNC-PMIC 144: L = 1435, H = 769.
UNC-PMIC 145: L = 1402, H = 769.
UNC-PMIC 146: L = 1448, H = 772.
UNC-PMIC 147: L = 1446, W = 670.
LJ — Females: L = 1454 ± 74, H = 776 ± 37 (n = 16).

ECOLOGY AND DISTRIBUTION: *Riocypris sarsi* has been found until now in two Patagonian environments: a swamp near Santa Cruz River and the shallow Lake Los Juncos. The latter is a temporary environment, characterized by alkaline (pH = 10.5 ± 1.6) and cold (temperature = 11.2 ± 5.4 °C) waters, with moderate conductivity (0.6 ± 0.4 mS/cm) and moderate dissolved oxygen concentration (9.7 ± 2.1 mg/L). These values were recorded during the austral spring (November and December) of the years 2012–2013, around midday.

REMARKS: *Eucypris sarsi* was described by Daday in 1902, from samples of a swamp near Amenkelt, lower Santa Cruz River, Patagonia (about 50°S, 69°W). The author presented some general morphological features and illustrated the valve shape of adult females and juveniles. Later, Farkas (1972) re-examined the type material, confirming the taxonomic position of *E. sarsi* and elaborating new illustrations of the valves, the carapace and the furca. Martens and Behen (1994) considered *E. sarsi* a senior synonym of *Eucypris fontana* (Graf 1931); however, Díaz and Martens (2014) established in a theoretical discussion that they are two clearly different species.

Eucypris sarsi described by Daday (1902) and by Farkas (1972) and *R. sarsi* recorded in Los Juncos share several features: carapace elongated in lateral view, with greatest height on the first third of the valve; anterior end broadly rounded and posterior one slightly blunted; left valve overlaps right valve; in internal lateral view, left valve with selvage peripheral and right valve with selvage displaced inwardly; valve surface smooth in adults and ornamented in juveniles; teeth bristles on Mx third endite serrated; Ga being 1.6 longer than Gp; and Sa slightly longer than Sp. Additionally, both taxa were recorded in the same region, the Argentinean Patagonia. Based on the aforementioned evidence, we considered that both taxa are the same species; therefore, we propose the new combination *Riocypris sarsi* (Daday 1902). De Deckker (1981) re-described *E. fontana* based on material from Signy Island, Antarctic; however, the specimens illustrated did not resemble *E. fontana* and were more similar to *E. sarsi* (Díaz and Martens 2014) and therefore to *R. sarsi*. In fact, many of the characteristics of the appendages illustrated by De Deckker (1981) resembles those of *R. sarsi*, particularly the absence of seta c on the T1, the furca attachment shape, and the ornaments on juvenile valves. Likewise, both taxa presented similar seta lengths on A1, the bristles on third Mx endite serrated, and the T2 with seta d1 almost four

Fig. 7. *Riocypris sarsi* comb. nov., female. (A) A1 (UNC-PMIC 139). (B) A2 (UNC-PMIC 140). (C) MdCx (UNC-PMIC 138). (D) Md palp (UNC-PMIC 138). (E) RLO (UNC-PMIC 138). Scale bars = 100 μm. For abbreviations refer to the Materials and methods.

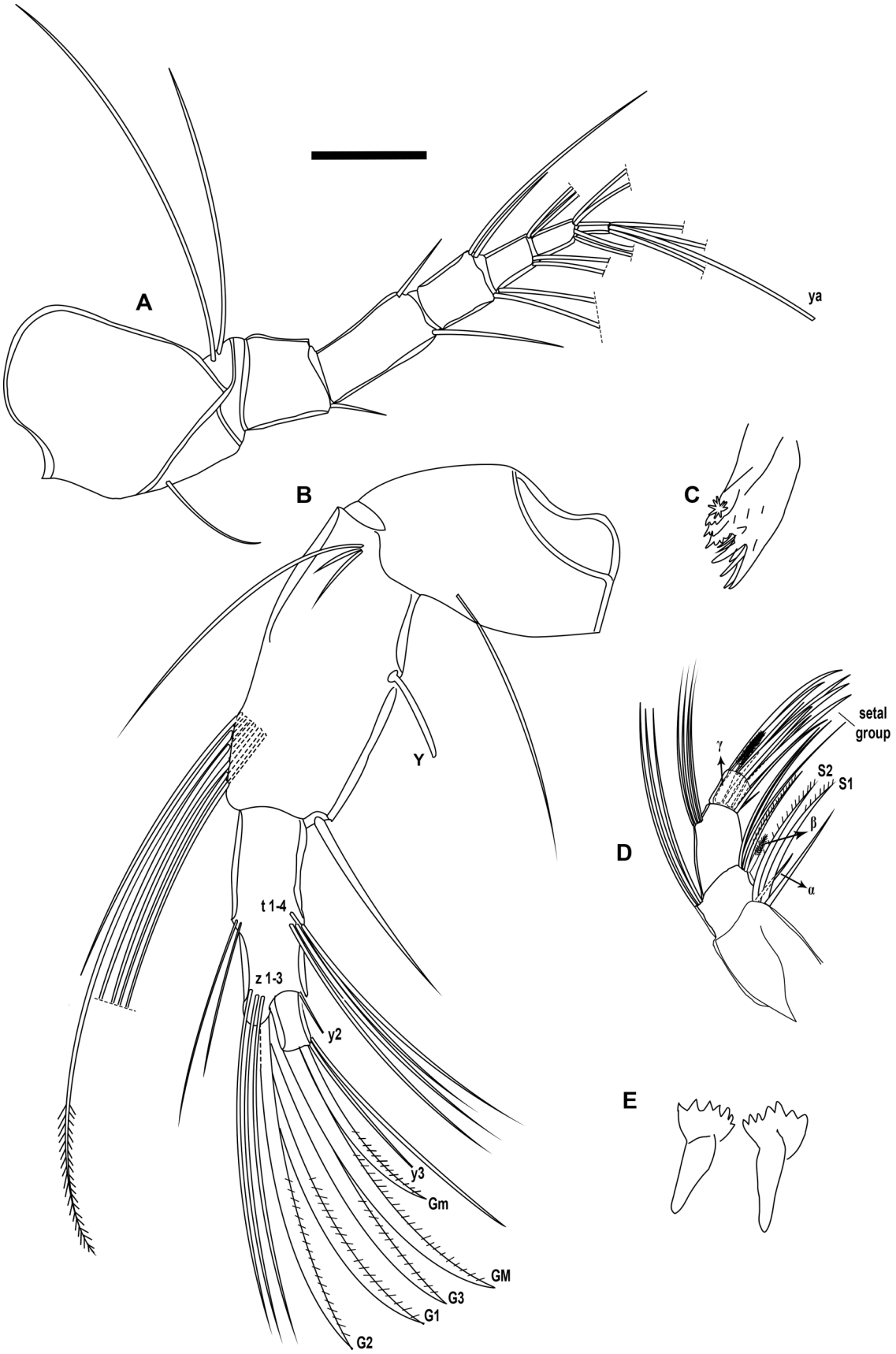

Fig. 8. *Riocypris sarsi* comb. nov., female. (A) Mx (UNC-PMIC 142). (B) T1 (UNC-PMIC 143). (C) T2 (UNC-PMIC 144). (D) T3 (UNC-PMIC 145). (E) CRa (UNC-PMIC 141). (F) CR (UNC-PMIC 141). Scale bar = 100 μm. For abbreviations refer to the Materials and methods.

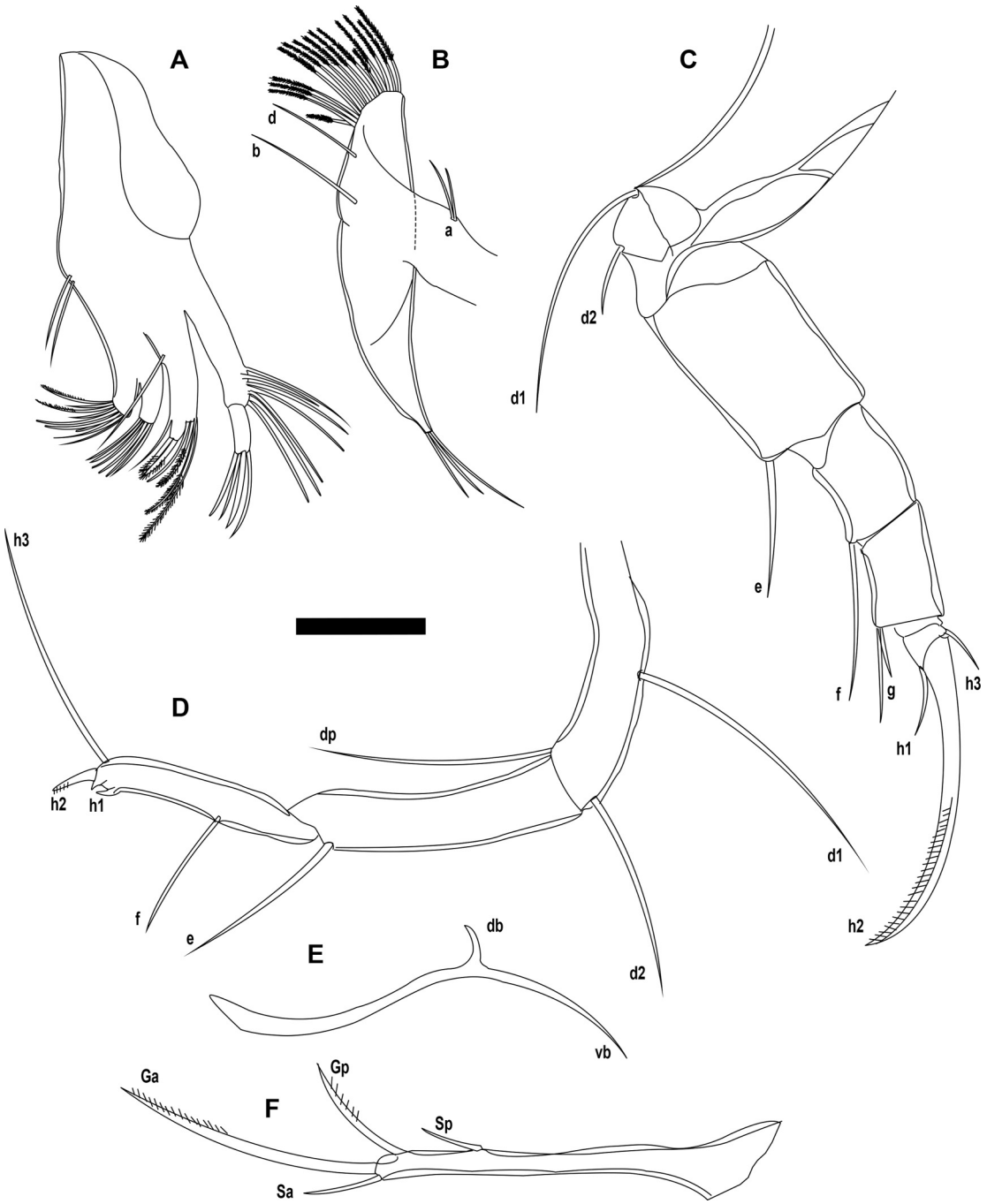

times as long as d1. However, De Deckker (1981) considered the absence of the anterior seta in the right furca as a diagnostic feature of his dissected specimens; this characteristic was not mentioned in the original *E. fontana* diagnosis (Graf 1931) and it is not presented in *R. sarsi*. In this context, De Deckker (1981) probably described a taxa close to *R. sarsi*.

Riocypris sarsi differs from *R. uruguayensis* in the shape of the carapace. The carapace of the latter is triangular in lateral view, with the greatest height situated in the middle of the valve; the anterior and posterior ends pointed, the dorsal margin more arched, and the ventral one more concave. In dorsal view, carapace distinctly beak-shaped in the anterior region. In *R. uruguayensis*, the short sixth seta of the second A2 endopodal segment is shorter, projecting beyond of the middle of the penultimate segment, whereas in *R. sarsi*, this seta reaches the distal end of the penultimate segment. In *R. uruguayensis*, the penultimate A2 segment is densely haired at its distal ventral corner, with setae on the ventral side finely spiked in the last 2/3 of its length. In this species, the last segment of Mx palp is less elongated (less than two times longer than wide in *R. uruguayensis*, whereas it is around two and a half times longer than wide in *R. sarsi*); the Sa on the caudal ramus is shorter, around 1/6 of length of Ga (in *R. sarsi*, Sa:Ga = 1/4); and the caudal ramus has setulae on the anterior margin (being smooth in *R sarsi*).

Riocypris sarsi differs from *R. hinzeae* in the size and shape of the carapace. The latter has a carapace subrectangular in lateral view,

Fig. 9. Nonmetric multidimensional scaling plot showing the shape dissimilarities between digitized outlines (normalized for area) of the left valves of *Riocypris whatleyi*, *Riocypris sarsi*, and *Eucypris fontana*. Colour version online. For abbreviations refer to the Materials and methods.

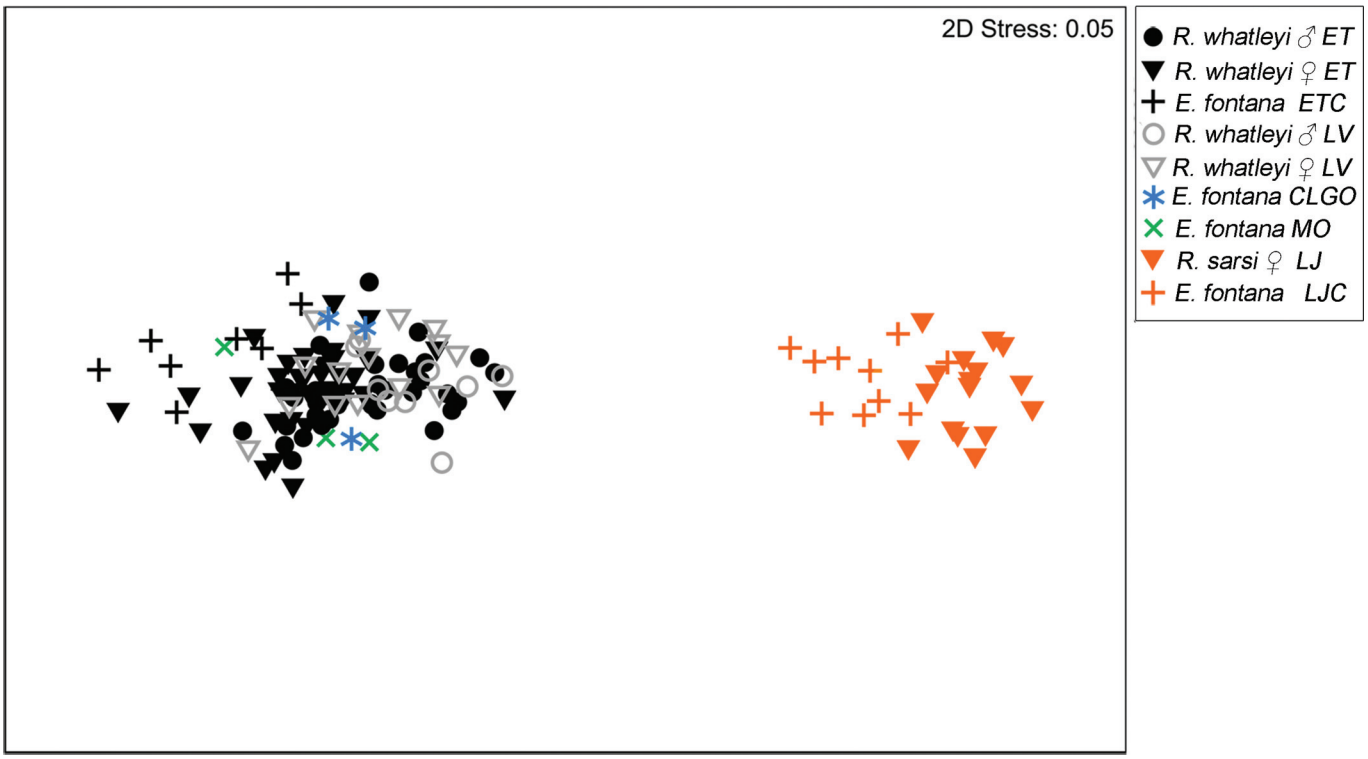

with anterior and posterior ends rounded and dorsal margin almost flat in the latter. In *R. hinzeae*, the second segment of the A1 is more elongated, the relationship d1/d2 in T2 is smaller (approximately three times in *R. hinzae* and four times in *R. sarsi*) and the Sa on the caudal ramus is very short, not reaching 1/7 of length of Ga (in *R. sarsi*, Sa around 1/4 of the length of Ga).

Riocypris sarsi differs from *R. whatleyi* in the shape of the carapace. The latter possesses a subtriangular carapace, with a dorsal valve margin substantially more arched and a more pronounced slope of the posterodorsal and anterodorsal margins; a greatest height in the middle of the valve and a greater H/L ratio (0.60 ± 0.01 (n = 98) in *R. whatleyi* and 0.54 ± 0.01 (n = 27) in *R. sarsi*); a posterior end rounded and a ventral margin straight to almost concave. In *R. whatleyi*, the dorsal seta on the A1 second segment exceeds the middle of the following segment (in *R. sarsi*, it reaches the base of the following segment), the last segment of Mx palp is less elongated (two times longer than wide in *R. whatleyi*, whereas it is around two and a half times longer than wide in *R. sarsi*), and the relationship and the ratio d1/d2 on T2 is higher (approximately five times in *R. whatleyi* and four times in *R. sarsi*).

Updated key to the species of the genus *Riocypris* (modified from Karanovic 2012 and Martens et al. 2013)

1. Dorsal margin evenly rounded, almost flat . . . . . *Riocypris hinzeae* Karanovic, 2008
— Dorsal margin highly arched 2
2. Dorsal margin triangular; anterior seta on caudal ramus very short, not reaching 1/5 of length of anterior claw . . . . . *Riocypris uruguayensis* Klie, 1935
— Dorsal margin subtriangular or weakly arched; anterior seta on caudal ramus reaching approximately 1/3 of length of anterior claw 3
3. Dorsal margin subtriangular, greatest H in the middle of the valve; dorsobasal seta on A1 reaching the third segment; relationship d1/d2 in T2 approximately five times . . . . . *Riocypris whatleyi* sp. nov.
— Dorsal margin slightly convex, greatest H situated in front of the middle; dorsobasal seta on A1 reaching the second segment; relationship d1/d2 in T2 approximately four times . . . . . *Riocypris sarsi* (Daday, 1902)

Geometric morphometric results

Shape analysis

Geometric morphometric analyses performed on *R. whatleyi* and *R. sarsi* showed a clear shape differentiation between both species (Fig. 9). The main shape differences are the dorsal valve margin: *R. whatleyi* is substantially more arched with a more pronounced slope of the posterodorsal and anterodorsal margins than *R. sarsi* (Fig. 10A). These shape differences were statistically significant (ANOSIM, R_{global} = 1, p = 0.1%). *Riocypris whatleyi* did not present interspecific morphological variability. They overlap in morphospace (Fig. 9) and the differences were not statistically significant (ANOSIM, R = 0.181, p = 0.2%). Valve outlines of males and females also overlap in morphospace (Fig. 9) and sexual dimorphism in shape was not statistically significant (ANOSIM, R = 0.092, p = 0.2%). The *E. fontana* specimens recovered from ETC, CLGO, and MO overlap in the *R. whatleyi* morphospace, and valves from LJC are more similar in shape to *R. sarsi* (Fig. 9).

Size analysis

Adult female valve size of *R. whatleyi* was larger than *R. sarsi* ($t_{[65]}$ = 10.2, p < 0.001). Both populations of *R. whatleyi* (ET and LV),

Fig. 10. Superposition of the virtual mean outline (consensus shape) of the *Riocypris whatleyi* from ET and LV and *Riocypris sarsi* from LJ. (A) Valve outlines were standardized for size (normalized for area) and positions. (B) Female valve outlines were not normalized for area. For abbreviations refer to the Materials and methods. Colour version online.

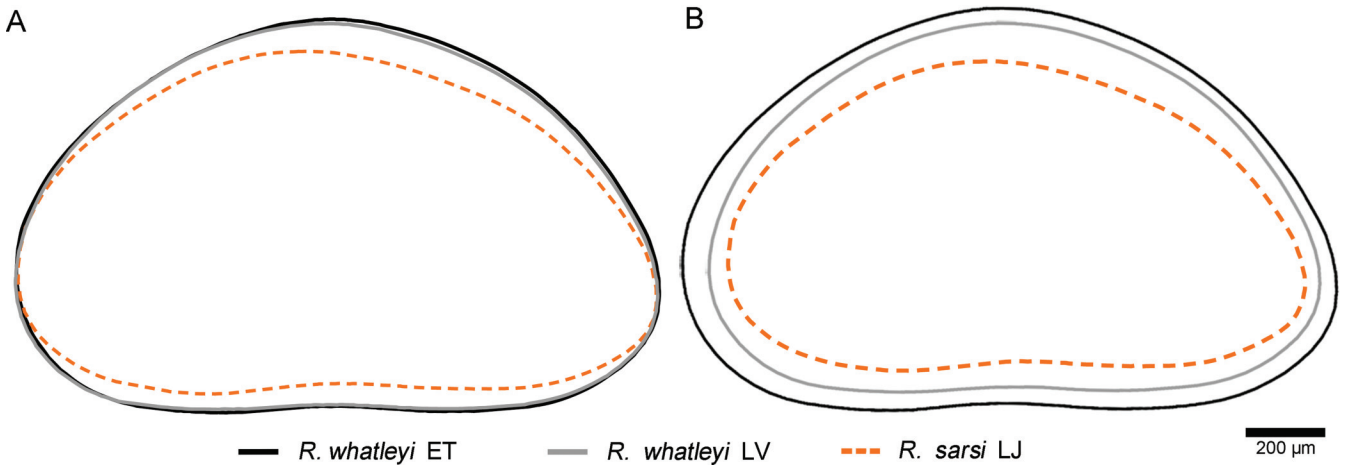

on average, had 16% larger valve size (1683 ± 80 µm, mean ± SD) than *R. sarsi* recovered from LJ lake (1453 ± 74 µm, mean ± SD) (Fig. 10B). Including the specimens recovered from cores (ETC and LJC) and outcrops (MO and ClGO), it was also found that the valves assigned as species *R. whatleyi* by the n-MDS (1622 ± 88, mean ± SD) are longer than those classified as *R. sarsi* (1446 ± 60, mean ± SD) (Mann–Whitney test, $Z_{adjusted} = 7.14$, $p < 0.001$).

In *R. whatleyi*, valve size differences between sites ($F_{[1,94]} = 213$, $p < 0.00001$) and sex ($F_{[1,94]} = 125.5$, $p < 0.00001$) were found. Females from ET, as well as from LV, have 8% and 3% larger valve size, respectively, than males of those sites (Fig. 11). Although an interaction between the effect of site (i.e., ET and LV) and sex on valve length was found ($F_{[1,94]} = 20.9$, $p < 0.001$), the amount of these interactions was low. This result indicates that there is an effect of both sex and site (i.e., ET or LV) on the size of the valves (Fig. 11). In summary, our findings show that the ET specimens are larger and that females are longer than males, although this is less evident in the LV site.

Discussion

The genus *Riocypris* belongs to the subfamily Cyprinotinae and is differentiated within the subfamily by the absence of tubercles along the valve margins and the presence of both seta d1 and seta d2 on the basal segment of the walking leg (Karanovic 2012). This genus was described by Klie (1935) in Uruguay, with *R. uruguayensis* as the type species. More recently, Karanovic (2008) reported the second species of this genus from wells in the Murchison region, western Australia. In the present contribution, two species of the genus *Riocypris* are described: *Riocypris whatleyi* and *Riocypris sarsi*. Both taxa were assigned to this genus by their inwardly displaced selvage on their right valve, a peripherical selvage on their left valve, and a prominent inner list; cylindrical maxillular palp; asymmetrical prehensile palps; absence of c seta on the first thoracopod; presence of both d setae (d1 and d2) on the walking leg; presence of a divided penultimate segment on the same appendage; and a thin and elongated caudal ramus, with both claws and setae present.

Riocypris whatleyi and *R. sarsi* differ both in the morphology of the valves and in the characteristics of the appendages. Morphological outline analysis has been previously used to distinguish different species (i.e., Mazzini et al. 2014). In this context, the valve outline analysis carried out in this work revealed that the differences between *R. whatleyi* and *R. sarsi* are clearly discontinuous, as they are widely separated in morphospace (Fig. 9). Additionally, significant differences in valve outlines of both taxa were found: *R. sarsi* shows a less arched dorsal margin than *R. whatleyi*, and these shape differences are even more evident when outlines were normalized for area (Figs. 10A, 10B). In the last decade, outline analysis has been used to identify nonmarine species successfully (Iepure et al. 2008; Ligios and Gliozzi 2012; Mazzini et al. 2014, 2015). Based on our comparative geometric morphometric analysis of living individuals dissected in this work and Quaternary specimens recovered from previous studies, we propose a taxonomic reassignment of those specimens originally determined as *E. fontana* in Patagonia. In particular, we suggest that the individuals assigned as *E. fontana* in Whatley and Cusminsky (1999, 2000), Schwalb et al. (2002), Cusminsky et al. (2005, 2011), Ramos et al. (2015), and Coviaga et al. (2017, 2018), characterized by an arched dorsal margin and the greatest height at the middle of the valve, correspond to *R. whatleyi*. The specimens assigned as *E. fontana* in Cusminsky and Whatley (1996: fig. 9) and Cusminsky et al. (2005: pl. 1, fig. 18), all of them with a slightly convex dorsal margin and the greatest height in front of the middle, correspond to *R. sarsi*. This reassignment has strong implications for paleoenvironmental reconstructions in Patagonia and point out that outline shape analysis would be a useful tool in the morphology-based differentiation process. Usually, only the ostracod carapace is preserved in the sediments, so its taxonomic identification in the paleontological record can be challenging (Torres Saldarriaga and Martinez 2010). Therefore, identification of living individuals (i.e., with valves and appendages) becomes an excellent tool for elucidating the taxonomic status of the different specimens in lacustrine sequences (Coviaga et al. 2018). A deeper understanding of the systematic and autecology of the taxa involved in paleoenvironmental studies is essential for carrying out precise interpretations of the associations preserved in the sediments. This knowledge would allow the identification and description of environmental changes and past climates (Torres Saldarriaga and Martínez 2010; Ramón-Mercau et al. 2012; Lorenschat and Schwalb 2013; Coviaga et al. 2017).

The Patagonian *E. fontana* specimens, hereinafter referred to as *R. whatleyi* and to *R. sarsi*, are widely distributed in Patagonia. Both species are common in recent assemblages and in Quaternary sequences, being frequently employed in ecological and paleoenvironmental studies (e.g., Cusminsky and Whatley 1996; Markgraf et al. 2003; Cusminsky et al. 2005, 2011; Ramón-Mercau et al. 2012; Coviaga et al. 2017, 2018). *Riocypris whatleyi* and *R. sarsi* have been recorded in ephemeral and permanent environments. However, *R. whatleyi* reaches its maximum abundance in permanent lakes (Markgraf et al. 2003; Cusminsky et al. 2005, 2011; Coviaga et al.

Fig. 11. Boxplot showing the valve length of *Riocypris whatleyi* for different sites (i.e., ET and LV) and sexes (i.e., male (♂) and female (♀)). Inset shows the superposition of digitalized outlines (not normalized for area) of left male (grey in print or light blue online) and female (black) valves of *R. whatleyi* from ET and LV. For abbreviations refer to the Materials and methods. Colour version online.

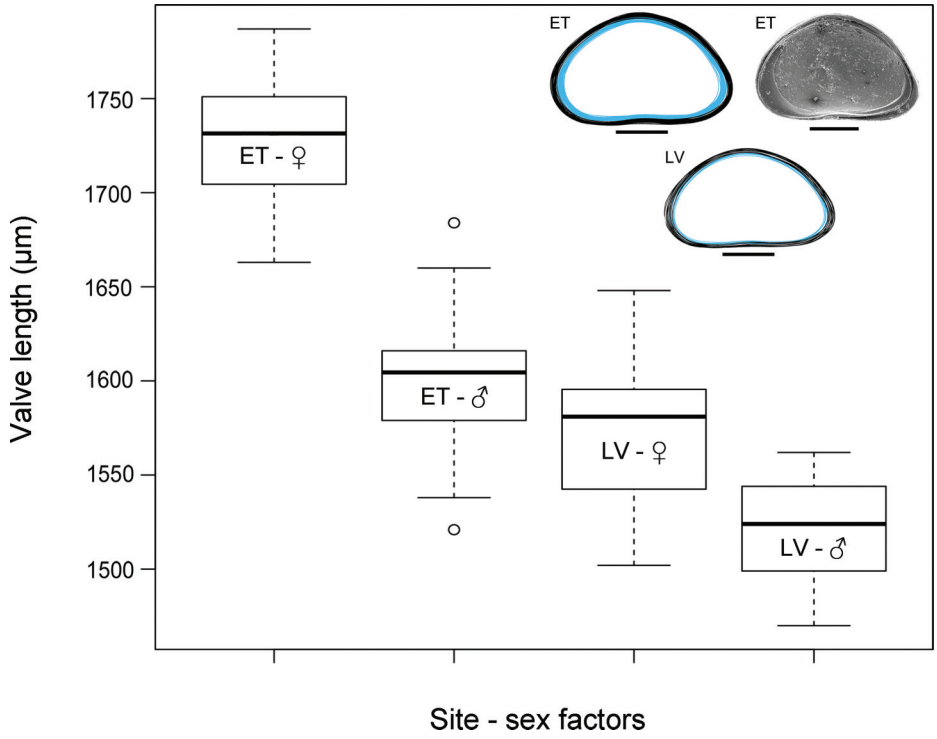

2018), whereas *R. sarsi* reaches its maximum abundance in temporary environments (Coviaga et al. 2018). Our results show that *R. whatleyi* is a limnetic to mesohaline species, capable of inhabiting waters with a wide range of solute composition and salinity, which has also reported by previous studies (Schwalb et al. 2002; Cusminsky et al. 2005; Ramón-Mercau et al. 2012; Ramón-Mercau and Laprida 2016; Coviaga et al. 2018). Nevertheless, this taxon prefers moderately saline conditions (optimal salinity estimated at 8686 µS/cm; Coviaga et al. 2018). *Riocypris sarsi*, however, is a limnetic taxa with preferences for water conductivity around 1000 µS/cm (Coviaga 2016).

Riocypris whatleyi populations from La Vertiente and El Toro have shown a significant size difference. This size variation may be caused by environmental factors such as water conductivity. This seems to be the case for *R. whatleyi*, which reached the largest dimensions (1663 ± 73 µm) in Lake El Toro under high conductivity conditions (30.1 ± 22.3 mS/cm), whereas Lake La Vertiente (low conductivity at 1.5 mS/cm) provided the smallest individuals (1552 ± 47 µm). Studies developed in Patagonia reported a positive relationship between the size of *Cypris pubera* O.F. Müller, 1776 and *Limnocythere rionegroensis* Whatley and Cusminsky, 1996 and conductivity (Coviaga et al. 2015; Ramos et al. 2017). However, the relationship between carapace size and salinity is complex and ostracods do not show a clear pattern of response (Yin et al. 1999); it is necessary to obtain additional data to evaluate this relationship within the *Riocypris* species and related taxa.

Sexual dimorphism in size was evaluated for *R. whatleyi*, the males being slightly smaller than the females. However, a clear discrimination between females and males was not possible based solely on valve outlines. Sex is not a unique factor determining the size of adult *R. whatleyi*. Additionally, the population to which specimens belong seems to mask the sexual dimorphism of this species, as suggested by the interaction found between site and sex factors. Ramos et al. (2015) described the same phenomenon in a previous study of *E. fontana*, where sexual dimorphism was not perceived when valves from different sites were considered a single cluster. These results have new implications in the analysis of fossil assemblages. However, like in other ostracod species, e.g., *Limnocythere inopinata* (Baird, 1843) (Roberts et al. 2002), variations in size over a geological time scale are also expected; therefore, the *R. whatleyi* sex classification based on size differences in fossil sequence could present further challenges.

The similarity between *R. whatleyi* and *Argentocypris sara* Díaz and Martens, 2014 valves is worth mentioning. Both species present a similar shape, with a clear anterior selvage in the right valve and similar distribution of wart-like elevations (*porenwarzen*?). Nevertheless, the appendicular morphology is quite different. The major difference between both taxa is the absence of the c seta on the T1 in *R. whatleyi*. This character has an important diagnostic value, being considered the most significant synapomorphy of the tribe Eucypridini Bronstein, 1947 (Martens 1989; Meisch 2000; Karanovic 2012; Díaz and Martens 2014). Consequently, *R. whatleyi* does not belong to the tribe Eucypridini and therefore would not be related to the genus *Argentonycpris*. Due to the three-dimensional nature of the first thoracopod and its relatively weak chitin, it is common for parts to fold over each other in a preparation and therefore the c seta is a very difficult characteristic to discern. It is therefore important to check its presence or absence in several specimens (Díaz and Martens 2014). Nevertheless, after having reviewed 36 specimens belonging to *R. whatleyi* and 11 belonging to *R. sarsi*, we are certain of the absence of c seta in the specimens employed in this study. Besides this difference, *R. whatleyi* presents other characteristics that do not match with the diagnostic characteristics of the genus *Argentocypris*: T2 with seta d1 almost three times as long as seta d2 (in *R. whatleyi*, it is approximately five times) and caudal ramus attachment with small db and vb and main branch curved over almost 180° (in *R. whatleyi*, the caudal ramus attachment with well-developed vb and very short db and main branch slightly curved). The *Riocypris* species here described presented wart-like elevations (*porenwarzen*?) on the outside and

the inside of both valves, similar to those present in *A. sara*. These structures are present in most *Eucypris* species and are absent in the remaining genus of the tribe. The presence of *porenwarzen* has also been reported in some species of the subfamily Cypridinae (Martens 1990, 2007; Meisch 2000) and in the candonid *Candona quasiincarum* Karanovic and Datry, 2009 (Karanovic and Datry 2009). We lack conclusive evidence to determine if these structures are homologous. Therefore, we leave the denomination "wart-like elevations" for *Riocypris* species until a homology is unequivocally established.

Patagonia remains a poorly explored region, with several taxonomic incognitos that need to be solved. Particularly, the ostracod taxonomic study continues to be incipient, with many descriptions based exclusively on valve morphology. Given the paleontological nature of these studies, only the ostracod carapace has been recovered and studied. In this context, the use of living individuals (e.g., with valves and appendages) becomes an excellent tool for elucidating the taxonomic status of the different specimens in lacustrine sequences. A greater knowledge of the systematic and autecology of the species used as indicators in paleolimnological and paleoclimatological studies would present a more solid foundation for their use as indicator species in paleoecological reconstructions. The present work is a contribution in that sense, increasing knowledge about the ostracod diversity in Patagonia and elucidating the taxonomic position of Patagonian *E. fontana*, a species widely used in paleoenvironmental studies in the region. Likewise, it highlights the usefulness of the simultaneous analysis of both recent and subfossil specimens, permitting an evidence-based use of this group as a modern analogue in paleoenvironmental studies.

Author contributions

C.C. and P.P. carried out the field sampling, the ostracods dissections, and conducted the taxonomical analysis. L.R. provided geometric morphometrics and statistical analyses. P.A. collaborated in the field sampling and developed the camera lucida illustrations. G.C. obtained the funding for this study and contributed with taxonomic descriptions and comparisons. C.C. wrote the manuscript, and all authors discussed the results and commented jointly on the manuscript.

Acknowledgements

We express our gratitude to M.A. Contreras and E. Macagno for their English revisions. We especially thank the owners and workers of the properties that we visited during sampling and the technical support of P. Troyón in MEB photos. We are also grateful to D. Zhai and two anonymous reviewers for their valuable comments that improved the manuscript. This work was supported by the National Council of Science and Technology Research of Argentina, CONICET under grants PIP 00819 and PIP 0021; the National Agency for the Promotion of Science and Technology under grants PICT 0082 and PICT 2014-1271; and the National University of Comahue under grants UNCo 04/B166 and UNCo 4/B194.

References

Baltanás, A., and Danielopol, D.L. 2011. Geometric morphometrics and its use in ostracod research: a short guide. Joannea Geol. Palaontol. **11**: 235–272.

Broodbakker, N.W., and Danielopol, D.L. 1982. The chaetotaxy of Cypridacea (Crustacea, Ostracoda) limbs: proposals for a descriptive model. Bijdragen tot de Dierkunde, **52**: 103–120.

Clarke, K.R., and Gorley, R.N. 2006. PRIMER v6: user manual/tutorial. PRIMER-E, Plymouth, U.K.

Clarke, K.R., and Warwick, R.M. 2001. Change in marine communities: an approach to statistical analysis and interpretation. Plymouth Marine Laboratory, Plymouth, U.K.

Coviaga, C. 2016. Ostrácodos lacustres actuales de Patagonia Norte y su correspondencia con secuencias holocénicas. Ph.D. thesis, Universidad Nacional del Comahue, San Carlos de Bariloche, Argentina.

Coviaga, C., Cusminsky, G., Baccalá, N., and Pérez, A.P. 2015. Dynamics of ostracod populations from shallow lakes of Patagonia: life history insights. J. Nat. Hist. **49**: 1023–1045. doi:10.1080/00222933.2014.981310.

Coviaga, C.A., Rizzo, A., Pérez, P., Daga, R., Poiré, D., Cusminsky, G., and Ribeiro Guebara, S. 2017. Reconstruction of the hydrologic history of a shallow Patagonian steppe lake during the past 700 yr, using chemical, geologic, and biological proxies. Quat. Res. **87**: 208–226. doi:10.1017/qua.2016.19.

Coviaga, C.A., Cusminsky, G.C., and Pérez, A.P. 2018. Ecology of freshwater ostracods from Northern Patagonia and their potential application in paleoenvironmental reconstructions. Hydrobiologia, **816**(1): 3–20. doi:10.1007/s10750-017-3127-1.

Cusminsky, G.C., and Whatley, R.C. 1996. Quaternary non-marine ostracods from lake beds in northern Patagonia. Rev. Esp. Paleontol. **11**: 143–154.

Cusminsky, G.C., Pérez, A.P., Schwalb, A., and Whatley, R. 2005. Recent lacustrine ostracods from Patagonia, Argentina. Rev. Esp. Paleontol. **37**(3): 431–450.

Cusminsky, G., Schwalb, A., Pérez, A.P., Pineda, D., Viehberg, F., Whatley, R., Markgraf, V., Gilli, A., Ariztegui, D., and Anselmetti, F.S. 2011. Late quaternary environmental changes in Patagonia as inferred from lacustrine fossil and extant ostracods. Biol. J. Linn. Soc. **103**(2): 397–408. doi:10.1111/j.1095-8312.2011.01650.x.

Daday, E.V. 1902. Mikroskopische-susswasserthiere aus Patagonien. Természetrajzi Füzetek, **25**: 201–313.

De Deckker, P. 1981. On *Eucypris fontana* (Graf). *In* A stereo-atlas of ostracod shells. *Edited by* R.H. Bate, J.W. Neale, L.M. Sheppard, and D.J. Siveter. The British Micropalaeontological Society and Robertson Research International Ltd., Llandudno, Wales, U.K. Vol. 8. pp. 87–92.

Díaz, A.R., and Martens, K. 2014. On *Argentocypris sara* gen. nov., sp. nov. (Ostracoda) from the Patagonian wetlands of Argentina. Crustaceana, **87**: 513–530. doi:10.1163/15685403-00003300.

Farkas, H. 1972. Data to the knowledge of *Eucypris sarsi* and *Erpetocypris obliqua* (Crustacea: Ostracoda). Ann. Hist.-Nat. Mus. Nat. Hung. **64**: 139–141.

Graf, H. 1931. Süsswasser Ostracoden aus Sudgeorgian. Zool. Anz. **93**: 185–191.

Horne, D.J., Cohen, A., and Martens, K. 2002. Taxonomy, morphology and biology of Quaternary and living Ostracoda. *In* The Ostracoda: applications in quaternary research. *Edited by* J.A. Holmes and A. Chivas. American Geophysical Union, Washington, D.C. pp. 6–36.

Iepure, S., Namiotko, T., and Danielopol, D.L. 2008. Morphological diversity and microevolutionary aspects of the lineage *Cryptocandona vavrai* Kaufmann, 1900 (Ostracoda, Candoninae). Ann. Limnol. Int. J. Lim. **44**: 151–166. doi:10.1051/limn:2008016.

Karanovic, I. 2008. Three interesting Cyprididae (Ostracoda) from Western Australia. Rec. West. Aust. Mus. **24**: 267–287. doi:10.18195/issn.0312-3162.24(3).2008.267-287.

Karanovic, I. 2012. Recent freshwater ostracods of the world. Springer, Berlin and Heidelberg. Available from http://link.springer.com/10.1007/978-3-642-21810-1.

Karanovic, I., and Datry, T. 2009. Overview of Candoninae (Crustacea, Ostracoda) of South America and the West Indies, with the description of two new species and one new genus. Zootaxa, **25**: 1–25. doi:10.11646/zootaxa.2267.1.1.

Klie, W. 1935. Süsswasser-Ostracoden aus Uruguay. Arch. Hydrobiol. **29**: 282–295.

Ligios, S., and Gliozzi, E. 2012. The genus *Cyprideis* Jones, 1857 (Crustacea, Ostracoda) in the Neogene of Italy: a geometric morphometric approach. Rev. Micropaleontol. **55**: 171–207. doi:10.1016/j.revmic.2012.09.002.

Linhart, J., Brauneis, W., Neubauer, W., and Danielopol, D.L. 2007. Morphomatica software, Version 1.6. Springer-Verlag, Berlin.

Lorenschat, J., and Schwalb, A. 2013. Autecology of the extant ostracod fauna of Lake Ohrid and adjacent waters — a key to paleoenvironmental reconstruction. Belg. J. Zool. **143**: 42–68.

Markgraf, V., Platt Bradbury, J., Schwalb, A., Burns, S.J., Stern, C., Ariztegui, D., Gilli, A., Anselmetti, F.S., Stine, S., and Maidana, N. 2003. Holocene palaeoclimates of southern Patagonia: limnological and environmental history of Lago Cardiel, Argentina. Holocene, **13**: 581–591. doi:10.1191/0959683603hl648rp.

Martens, K. 1987. Homology and functional morphology of the sexual dimorphism in the antenna of *Sclerocypris* Sars, 1924 (Crustacea, Ostracoda, Megalocypridinae). Bijdragen tot de Dierkunde, **57**: 183–190.

Martens, K. 1989. On the systematic position of the *Eucypris* clavata-group with a description of *Trajancypris* gen. nov. (Crustacea, Ostracoda). Arch. Hydrobiol. **83**: 227–251.

Martens, K. 1990. Taxonomic revision of African Cypridini. Part I: The genera of *Cypris* O.F. Müller, *Pseudocypris* Daday and *Globocypris* Klie (Crustacea, Ostracoda). Bull. Inst. R. Sci. Nat. Bel. Biol. **60**: 127–172.

Martens, K. 2007. On a new species and genus in the Cypridini (Crustacea, Ostracoda, Cyprididae) from South Africa, with a phylogenetic analysis of the tribe and a discussion on the genus concept in this group. J. Nat. Hist. **41**: 381–399. doi:10.1080/00222930601157183.

Martens, K., and Behen, F. 1994. A checklist of the recent non-marine ostracods (Crustacea, Ostracoda) from the inland waters of South America and adjacent islands. Trav. Sci. Mus. Nat. Hist. Nat. Luxemb. **22**: 1–81.

Martens, K., and Savatenalinton, S. 2011. A subjective checklist of the recent, free-living, non- marine Ostracoda (Crustacea). Zootaxa, **2855**: 1–79.

Martens, K., Schon, I., Meisch, C., and Horne, D.J. 2008. Global diversity of ostracods (Ostracoda, Crustacea) in freshwater. Hydrobiologia, **595**: 185–193. doi:10.1007/s10750-007-9245-4.

Martens, K., Savatenalinton, S., Schön, I., Meisch, C., and Horne, D.J. 2013. World checklist of freshwater Ostracoda species. Freshwater Animal Diversity As-

sessment (FADA) hosted on the Belgian Biodiversity Platform, Brussels. Available from http://fada.biodiversity.be/group/show/18.
Mazzini, I., Gliozzi, E., Rossetti, G., and Pieri, V. 2014. The *Ilyocypris* puzzle: a multidisciplinary approach to the study of phenotypic variability. Int. Rev. Hydrobiol. **99**: 395–408. doi:10.1002/iroh.201301729.
Mazzini, I., Gliozzi, E., Koci, R., Soulie-Märsche, I., Zanchetta, G., Baneschi, I., Sadori, L., Giardini, M., Van Welden, A., and Bushati, S. 2015. Historical evolution and Middle to Late Holocene environmental changes in Lake Shkodra (Albania): new evidences from micropaleontological analysis. Palaeogeogr. Palaeoclimatol. Palaeoecol. **419**: 47–59. doi:10.1016/j.palaeo.2014.08.012.
Meisch, C. 2000. Freshwater Ostracoda of western and central Europe. Süßwasserfauna von Mitteleuropa 8/3. Spektrum Akademischer Verlag, Heidelberg.
Mischke, S., BöBneck, U., Diekmann, B., Herzschuh, U., Jun, H., Kramer, A., Wünnemann, B., and Zhang, C. 2010. Quantitative relationship between water-depth and sub-fossil ostracod assemblages in Lake Donggi Cona, Qinghai Province, China. J. Paleolimnol. **43**: 589–608. doi:10.1007/s10933-009-9355-2.
Neubauer, W., and Linhart, J. 2008. Approximating and distinguishing Ostracoda by the use of B-Splines. *In* Contribution to geometric morphometrics. *Edited by* D.L. Danielopol, M. Gross, and W.E. Piller. Karl Franzens Universität, Graz, Austria. pp. 21–42.
Ohlendorf, C., Fey, M., Massaferro, J., Haberzettl, T., Laprida, C., Lücke, A., Maidana, N., Mayr, C., Oeherich, M., Ramón-Mercau, J., Wille, M., Corbella, H., St-Onge, G., Schäbitz, F., and Zolitschka, B. 2014. Late Holocene hydrology inferred from lacustrine sediments of Laguna Cháltel (southeastern Argentina). Palaeogeogr. Palaeoclimatol. Palaeoecol. **411**: 229–248. doi:10.1016/j.palaeo.2014.06.030.
Ramón-Mercau, J., and Laprida, C. 2016. An ostracod-based calibration function for electrical conductivity reconstruction in lacustrine environments in Patagonia, southern South America. Ecol. Indic. **69**: 522–532. doi:10.1016/j.ecolind.2016.05.026.
Ramón-Mercau, J., Laprida, C., Massaferro, J., Rogora, M., Tartari, G., and Maidana, N. 2012. Patagonian ostracods as indicators of climate-related hydrological variables, implications for paleoenvironmental reconstructions in southern South America. Hydrobiologia, **694**: 235–251. doi:10.1007/s10750-012-1192-z.
Ramos, L.Y., Alperin, M., Pérez, A.P., Coviaga, C., Schwalb, A., and Cusminsky, G. 2015. *Eucypris fontana* (Graf, 1931) (Crustacea, Ostracoda) in permanent environments of Patagonia Argentina: a geometric morphometric approach. Ann. Limnol. Int. J. Limnol. **51**: 125–138. doi:10.1051/limn/2015007.
Ramos, L., Cusminsky, G., Schwalb, A., and Alperin, M. 2017. Morphotypes of the lacustrine ostracod *Limnocythere rionegroensis* Cusminsky & Whatley from Patagonia, Argentina, shaped by aquatic environments. Hydrobiologia, **786**(1): 137–148. doi:10.1007/s10750-016-2870-z.
Roberts, J.H., Holmes, J.A., and Swan, A.R.H. 2002. Ecophenotypy in *Limnocythere inopinata* (Ostracoda) from the late Holocene of Kajemarum Oasis (northeastern Nigeria). Palaeogeogr. Palaeoclimatol. Palaeoecol. **185**: 41–52. doi:10.1016/S0031-0182(02)00254-7.
Rohlf, F.J. 2010. TpsDig digitize landmarks from image files, scanner, or video. Version 2.16 [computer program]. Department of Ecology and Evolution, State University of New York at Stony Brook, Stony Brook.
Schaffer, B., Alford, R., Woodward, B., Richards, S., Altig, R., and Gascon, C. 1994. Quantitative sampling of amphibian larvae. *In* Measuring and monitoring biological diversity: standard methods for amphibians. *Edited by* W.R. Heyer, M.A. Donnelly, R.W. McDiarmid, L.C. Hayek, and M.S. Foster. Smithsonian Institution Press, Washington, D.C. pp. 130–141.
Schwalb, A.J., Burns, S., Cusminsky, G., Kelts, K., and Markgraf, V. 2002. Assemblage diversity and isotopic signals of modern ostracodes and host waters from Patagonia, Argentina. Palaeogeogr. Palaeoclimatol. Palaeoecol. **187**: 323–339. doi:10.1016/S0031-0182(02)00484-4.
StatSoft, Inc. 2004. STATISTICA. Version 7.0 [computer program]. StatSoft, Inc., Tulsa, Okla.
Torres Saldarriaga, A., and Martínez, J.I. 2010. Ecology of non-marine Ostracoda from La Fe Reservoir (El Retiro, Antioquia) and their potential application in paleoenvironmental studies. Rev. Acad. Colomb. Cienc. Exactas Fis. Nat. **34**: 397–409.
Vavra, W. 1898. Süsswasser-Ostracoden. Ergebn. Hamburger Magalh. Sammelreise 1892–1893, Naturhist. Mus. Hamburg (Ed.). Vol. 2. pp. 1–26.
Whatley, R.C., and Cusminsky, G.C. 1999. Lacustrine Ostracoda and late Quaternary palaeoenvironments from the Lake Cari-Laufquen region, Rio Negro province, Argentina. Palaeogeogr. Palaeoclimatol. Palaeoecol. **151**: 229–239. doi:10.1016/S0031-0182(99)00022-X.
Whatley, R.C., and Cusminsky, G.C. 2000. Quaternary lacustrine Ostracoda from northern Patagonia: a review. *In* Lake basins through space and time. *Edited by* E.H. Gierlowski-Kordesch and K.R. Kelts. AAPG Stud. Geol. **46**: 581–590.
Yin, Y., Geiger, W., and Martens, K. 1999. Effects of genotype and environment on phenotypic variability in *Limnocythere inopinata* (Crustacea: Ostracoda). Hydrobiologia, **400**: 85–114. doi:10.1023/A:1003759125903.
Zhang, W., Mischke, S., Zhang, C., Gao, D., and Fan, R. 2013. Ostracod distribution and habitat relationships in the Kunlun Mountains, northern Tibetan Plateau. Quat. Int. **313–314**: 38–46. doi:10.1016/j.quaint.2013.06.020.